AIR PRESSURE ENERGY STORAGE FOR REVERSE OSMOSIS: BENCH-SCALE PROOF OF CONCEPT

A Thesis
Presented to
the Graduate School of
Clemson University

In Partial Fulfillment
of the Requirements for the Degree
Master of Science
Environmental Engineering and Science

---

by
Ying Sun
August 2013

Accepted by:
Dr. David Ladner, Committee Chair
Dr. Fred Molz
Dr. Thomas Overcamp

ABSTRACT

Society faces diminishing access to clean drinking water because of increasing global population and the development of modern industries. At the same time, climate change and other environmental problems caused by the increase in fossil fuel consumption the emphasis on reducing dependency on traditional energy resources in the process of potable water production. To address both problems, a small-scale wind powered reverse osmosis (RO) desalination system with a unique energy storage mechanism was envisioned to provide an energy buffer such that fluctuating and intermittent wind can be utilized. Energy is stored in the form of compressed air in a pressure vessel (PV).

The feasibility of this innovative design was evaluated for both seawater (35 g/l and 45 g/L NaCl solutions were selected for seawater experiments) and brackish water (15 g/L and 25 g/L NaCl solutions were selected for brackish water experiments) desalination. The RO desalination coupled with the PV energy storage device was tested using bench-scale experiments under different operating conditions. It was found that high initial air pressure can help to produce the greatest flux and good water quality (>98.6% salt rejection), while different crossflow speeds did not affect the performance of energy-buffered experiments. The performance was further tested with simulated fluctuating and intermittent wind speeds to mimic real-world conditions. It was demonstrated that the energy storage tank can largely dampen the variability in applied pressure and discharge rate caused by wind fluctuation and significantly improve the desalination performance for both flux and rejection without any pressure control strategy.

Since high quality drinking water (>98.6% salt rejection) was produced under applied pressure as low as 700 psi, the applied pressure could be lowered to reduce energy consumption. Under simulated intermittent wind operation, RO desalination with energy storage showed significant advantage over traditional RO desalination (with no energy storage mechanism) in that PV can store the energy when the wind dies down and the stored energy can be used to produce good quality drinking water when a small amount of energy is available to provide crossflow. The effects of dissolved nitrogen under high pressure on the RO process were also evaluated. The experimental results indicated that comparing with conventional RO, the RO process with PV did not show a consistent benefit or detriment in flux using different feed concentrations from 0 to 45 g/L, but caused a slight improvement on rejection for all feed concentrations.

DEDICATION

This thesis is dedicated to my parents, Mr. Gang Sun and Mrs. Xiuhua Mao, and my husband, Mr. Lei Zhu for their love, endless support and encouragement.

ACKNOWLEDGMENTS

It would not have been possible to write this master's thesis without the guidance and support of many people around me. Foremost, I would like to thank my research adviser, Dr. David Ladner, for the mentorship and guidance he provided to me. He helped me to gain practical knowledge and research experience which led my way to get my career started. He has always been very understanding and stood by my side when I met unsolved issues during studying at Clemson University and interning in San Francisco. He is not only a great advisor, but also a true friend. Besides my advisor, I would like to thank Dr. Tanju Karanfil and Dr. Thomas Overcamp for serving as my research committee.

I also would like to acknowledge the financial, academic and technical support of Department of Environmental Engineering and Earth Sciences at Clemson University. I would like to thank Mrs. Anne Cummings and Mr. Kenneth E. Dunn for their help in setting up the bench scale system presented in this document.

I would like to thank my fellow labmates in membrane group: Pooja Mahajan, Pengxie, Muriel Steele, Dan Carey, Erin Partlan, Jaclyn Ellerie, Minjie Zhou and Megan Smith, for the stimulating discussions and all the fun we have had in the last two years. In particular, I am grateful to my co-worker, Pooja Mahajan for performing modeling the experiments I conducted and the enlightening conversation we had.

My sincere thanks also goes to Mrs. Doris Wilson, Mr. Alex Miot and Mrs. Manisha Berde for offering me the student internship opportunities, leading me working

on diverse exciting projects and helping me gain real world experience at three wastewater treatment plants in South Carolina and California.

Last but not the least, I would like to thank my husband, Lei Zhu, for his personal support and being with me through tough times. My parents, Mr. Gang Sun and Mrs. Xiuhua Mao, have given me their unequivocal support and understanding through all my life.

TABLE OF CONTENTS

Page

Table of Contents (Continued)

Page

LIST OF TABLES

Table Page

LIST OF FIGURES

Figure Page

List of Figures (Continued)

Figure Page

NOMENCLATURE

M_p	Accumulated permeate mass
P_b	Batch mode pressure in the PV
BWRO	Brackish water reverse osmosis
L	Constant describing the physical characteristics of the membrane
CRO	Conventional reverse osmosis
ρ_f	Density of feed solution
ρ_N	Density of nitrogen
ED	Electrodialysis reversal
FS	Freeze Separation
GHG	Greenhouse gas
μ	Liquid viscosity
lmh	Liters/m^2/h
MED	Multiple effects desalination
MED-TVC	Multi-effect distillation with thermal vapor compression
MSF	Multi-stage flash distillation
MVC	Mechanical vapor compression
C_N	Nitrogen concentration in salt water
$\Delta \pi$	Osmotic pressure
f_{os}	Osmotic pressure factor
PV	Pressure vessel
Rc	Resistance of the cake

Rm	Resistance of the membrane
RO	Reverse osmosis
SWRO	Seawater reverse osmosis
SD	Solar distillation
P_s	Steady state applied pressure
TDS	Total dissolved solids
ΔP	Transmembrane pressure
VC	Vapor compression
V_{air}	Volume of air in the PV
V_f	Volume of feed in feed tank
V_i	Volume of initial feed solution
V_{pv}	Volume of the PV
V_{sw}	Volume of salt water in the PV
N_{Aw}	Water flux
WRO	Wind reverse osmosis

CHAPTER 1 INTRODUCTION

Diminishing access to freshwater resources has led to growing interest in saltwater reverse osmosis (RO) desalination. Energy intensity requirements remain a drawback in RO desalination as energy costs and depleting natural resources are of concern. Renewable wind energy is a promising alternative to drive RO desalination because of its relatively low environmental impact and potential energy cost savings. The challenge lies in using fluctuating and intermittent wind energy to drive the RO desalination process, which benefits from a steady power source. In order to address both freshwater shortage and conventional energy scarcity crises, an innovative wind driven RO desalination process with a unique energy storage device was designed to enable efficient RO operation using intermittent and fluctuating power. This thesis project is to evaluate the feasibility of this unique wind RO system for both seawater (35 g/L and 45 g/L NaCl solutions were selected for seawater experiments) and brackish water (15 g/L and 25 g/L NaCl solutions were selected for brackish water experiments) desalination using bench-scale laboratory experiments.

The main hypothesis of this work is that the RO system coupled with an energy storage device would result in more stabilized operation, greater permeate generation, higher salt rejection and less energy consumption when a variable energy source, such as a wind turbine is utilized. Different operating conditions including feed concentration, crossflow velocities, and initial air pressure were tested to obtain optimal operation conditions in order to produce maximum flux and water quality while optimizing energy consumption. The performance of this system with energy storage, acting as an energy

buffer, was further tested with fluctuating and intermittent wind speeds to simulate real-world conditions. The effect of dissolved air in the feed on the performance was also explored. The comparison with traditional RO desalination (with no energy storage mechanism) was made to see performance improvement of the RO desalination process under both steady-state and wind-RO (fluctuating and intermittent) conditions.

CHAPTER 2 LITERATURE REVIEW

Seawater and brackish water desalination is becoming a promising treatment technology to provide municipal drinking water as freshwater demand increases. However, the main drawback of current desalination processes is high energy demand, which causes high operating costs. At the same time, high consumption of fossil fuels increases the negative effects of desalination on the environment. Therefore, desalination processes using renewable energies as power resources are fundamentally attractive. The drawback is that renewable sources are intermittent and low-intensity while RO membranes typically operate with continuous and high-intensity power. To enable renewable energies in desalination processes, it is useful to understand the demand of freshwater and the desalination technologies, as well as explore existing design, development and studies of renewable energy driven seawater desalination.

2.1. Increasing Demand for Freshwater

Society faces diminishing access to clean drinking water because of increasing global population, development of modern industries, irrational waste and especially severe contamination of existing resources (Charcosset 2009; Mathioulakis et al. 2007; Mohamed and Papadakis 2004; Raluy et al. 2005; Tarnacki et al. 2012). These factors amplify the emphasis placed on potable water production and its technologies.

From the U.S. Geological Survey, 96.5% of Earth's water is located in seas and oceans, 1.7% of Earth's water is bound in ice and only approximately 0.8% is considered to be freshwater (Greenlee et al. 2009). The accessible freshwater lakes and rivers contain a little more than 0.25% of total freshwater, while the rest is underground or is bound in

glaciers (Kalogirou 2005). The remaining percentage is made up of brackish water and slightly salty water mainly found as surface water in estuaries and as groundwater in salty aquifers (Greenlee et al. 2009). Among those, freshwater is the main resource used in daily life and industrial processes, while a large percentage of seawater and brackish water remain unused.

Traditional freshwater resources such as lakes, rivers, and groundwater are overused or misused. With development of modern societies, few new freshwater resources are available to support daily needs. But, demand for clean water is increasing due to world-wide population growth and the deteriorating quality of the existing potable resources (Carta et al. 2003). From 2000 to 2020, the population will increase about 50% in Africa, 25% in Asia, and 14% in the USA, even though there will be a 2% decrease in Europe (Eltawil et al. 2009). The population will increase dramatically over next decade or so, which will cause severe water shortages in the future, especially in most of the developing countries in Africa and Asia (Food and Agriculture Organization of the United Nations 2000). Today, about three billion people around the world are without clean drinking water and about 1.76 billion people live in areas with high degrees of water shortage (Charcosset 2009). According to the World Water Council, the world population will face a 17% freshwater shortage by 2020 (Gilau and Small 2008). Also, in inland areas, brackish water may be the only option, while at some coastal sites and remote areas, seawater may be the only water resource (Warfel et al. 1988). As a result, alternative solutions such as saltwater desalination have emerged as important tools to sustain future generations.

2.2. Reverse Osmosis Desalination Technologies

Desalination technology developed over 40 years has led to considerable reduction in investment costs, energy consumption, and advances in system design and operating experiences (Carta et al. 2003; Greenlee et al. 2009). In fact, desalinated seawater and underground saline water have become one of the main sources of water in some arid regions, coastal areas and remote islands where non-saline resources are not available (Carta et al. 2003). Thus, desalination can be considered as one method to satisfy increasing water demand.

Total dissolved solids (TDS) is commonly used to express salt concentration in water (Liu et al. 2002). Seawater has a TDS of 35,000 to 45,000 mg/l, while the TDS of brackish water is between 1000 mg/L and 10,000 mg/L (Liu et al. 2002). The potable water standard from the World Health Organization for sanitary water is below 500 mg/L of TDS, or about 2% seawater (World Health Organization 1973). Excess TDS causes taste and health problems, such as stomach illnesses and laxative effects (El-Ghonemy 2012). Therefore, desalination methods are needed to enable seawater/brackish water as drinking water.

Among various desalination technologies, RO has a 44% share in world desalting production capacity and an 80% share in the total number of desalination plants installed worldwide (Greenlee et al. 2009). From the data presented in Table 1, RO processes require less total energy than thermal desalination processes per unit volume of water treated. So from the aspect of energy consumption, RO is one of the most efficient desalination processes (Peñate and García-Rodríguez 2012). RO requires about 4.5-8.5

kWh and 1.0-2.5 kWh of energy per m^3 of fresh water produced from seawater and brackish water respectively (Ackermann and Söder 2002; Colombo et al. 1999; Peñate and García-Rodríguez 2012). Because of the energy efficiency, new membrane materials together with simplicity of design and availability of numerous manufacturers, RO is often chosen during the selection and design processes (Tarnacki et al. 2012; Veza 2001).

Table 2.2.1 Relative power requirements of desalination processes in 2000 (Eltawil et al. 2009).

Process	Electrical energy consumption (kWh/m^3)	Thermal energy consumption (kWh/m^3)	Total energy consumption (kWh/m^3)
BWRO[1]	1.0-2.5	N/A	1.0-2.5
SWRO[2]	4.5-8.5	N/A	4.5-8.5
MSF[3]	3.25-3.75	6.75-9.75	10.5-13
MED[4]	2.5-2.9	4.5-6.5	7.4-9
MED-TVC[5]	2.0-2.5	6.5-12	9-14
MVC[6]	9.5-17	N/A	9.5-17

[1] BWRO – Brackish water RO
[2] SWRO – Seawater RO
[3] MSF – Multi-stage flash
[4] MED – Multi-effect distillation
[5] MED-TVC – Multi-effect distillation with thermal vapor compression
[6] MVC – Mechanical vapor compression

In RO, a semi-permeable membrane separates two solutions with different concentrations (Fritzmann et al. 2007). The pressure differential that exceeds the natural osmotic pressure differential drives the process and determines the rate at which fresh water crosses the membrane (Abdallah et al. 2005, Eltawil et al. 2009). The major energy requirement is the initial pressurization of the feed water. The required pressure depends on the salt concentration of feed solution. The operating pressure is from 220 to 435 psi for brackish water desalination, while it is from 800 to 1015 psi for seawater desalination

(Abdallah et al. 2005). The feed water becomes concentrated as salts are retained. The recovery from feed water is limited in order to avoid fouling and to reduce energy costs. Seawater RO plants have recoveries from 25 to 45%, while brackish water RO plants have recovery rates as high as 90% (Charcosset 2009). In a relatively closed sea, like the Red Sea or the Persian Gulf, relatively low recovery is usually obtained (Charcosset 2009). Membrane modules, high-pressure pumps, energy generation plant and energy recovery devices (as needed) are the main components of an RO system. Membrane properties and salinity of the feed water are the two major factors controlling the energy requirements. More energy is required to overcome the osmotic pressure high water salinity.

The osmotic pressure difference between feed water and product water (or permeate) can be calculated by the following equation (Ladner et al. 2010):

$$\Delta \pi = f_{os} (TDS_{feed} - TDS_{product}) \quad [1]$$

Where $\Delta \pi$ is the transmembrane osmotic pressure (often in units of psi), f_{os} is the osmotic pressure factor and TDS is the total dissolved solids in units of mg/L.

Based on Eq. 1, the osmotic pressure is directly related to salt concentration. Use of brackish water as feed for the RO desalination process would give a smaller $\Delta \pi$ than seawater desalination and would require less energy.

In many remote areas, such as islands and isolated inland areas, seawater or brackish water may be the only economic water resources available. Under such circumstance, RO desalination is one of the most promising technologies for providing potable water. The electricity supply in those isolated areas may be a problem, thus,

renewable energy alternatives need to be considered (De Almeida and Moura 2007). Many advances have been achieved in RO membrane technologies through a few decades' development, such as improved pressure fluctuation tolerance and higher rejection rates, which make using inconstant renewable energy possible. But, use of RO in small stand-alone systems using renewable energies is still a developing technology. This will be discussed in detail in the next two sections.

2.3. Renewable Energy Desirability for RO Desalination

Recent attention has been given to renewable energy in the area of brackish and seawater desalination (Goosen et al. 2011). Many industrial countries are already in the position of increasing the share of renewable energy in their portfolios by supporting new technology expansion and market introduction. For example, the European Union has set a goal of doubling its renewable energy use by 2010 and recommended a worldwide carbon emission reduction of 75% by the end of the 21st century to prevent unpredictable negative effects on the global climate and economy (Charcosset 2009).

Energy consumption (Figure 2.3.1) remains the major operational cost for RO desalination, due to the high pressure pumps. The RO process consumes about 3-8 kWh/m^3 for freshwater production (De Almeida and Moura 2007), which is usually obtained through electricity from fossil fuels (Carta et al. 2003; Kamal and Tusel 1982; Subramani et al. 2011). Fossil fuels are exhaustible and produce various air pollutants, such as greenhouse gases, nitrogen dioxide and sulfur dioxide. Renewable energies, such as wind, solar, tidal and geothermal energies are inexhaustible and release few pollutants during operation (though pollutants may be emitted during equipment manufacturing), so

renewable energy systems offer alternative solutions which can significantly decrease the dependence of desalination on fossil fuels (Joselin Herbert et al. 2007). For RO seawater desalination driven by energy generated by traditional fossil fuel, CO_2 and NO_x emissions are 1.78 kg/m^3 and 4.05 g/m^3 of seawater treated, respectively (Subramani et al. 2011). When it comes to RO processes driven by wind, greenhouse gas emissions are much lower; in one case it was estimated that CO_2 and NO_x emissions were 0.1 kg/m^3 and 0.4 g/m^3, respectively (Subramani et al. 2011).

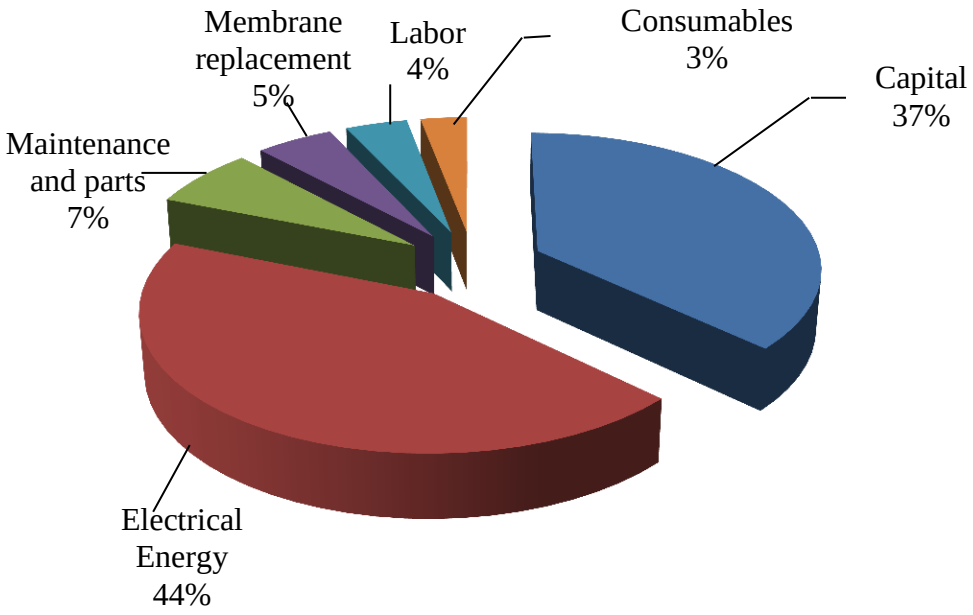

Figure 2.3.1 Typical cost structure for RO desalination of seawater (El-Ghonemy 2012)

In many remote areas with low-density populations, conventional energy resources are not accessible or are too expensive to afford, which makes renewable energy a potentially viable option for stand-alone desalination systems (Gude et al. 2010; Mathioulakis et al. 2007). Water production cost can be reduced to a great extent

compared with the costs of transporting water to these remote areas or using conventional fuels as a power source. Therefore, the motivation for using renewable energy is even greater under this situation.

Many different solutions have been proposed in the field of renewable energy driven desalination. There are several alternative configurations available with combinations of particular renewable sources with specific desalination processes. Table 2.3.1 shows a summary of the technically possible combinations of renewable energy sources and desalination techniques.

Table 2.3.1 Applicability of renewable energy sources to desalination processes (Hanafi 1994)

Wind	Solar	Tidal	Geothermal
RO[1]	RO	RO	RO
VC[2]	MSF[3]	VC	VC
FS[4]	ME[5]	FS	MSF
ED[6]	ED	ED	ED
	SD[7]		ME

[1] RO-Reverse osmosis
[2] VC-Vapor compression
[3] MSF-Multi-stage flash distillation
[4] FS-Freeze separation
[5] ME-Multiple effects desalination
[6] ED-Electrodialysis reversal
[7] SD-Solar distillation

Wind power is one of the most promising renewable energy options to couple with RO desalination units, especially for remote and coastal areas with good wind energy resources (Chen 2011; Subramani et al. 2011; Voivontas et al. 2001). Compared with other renewable energies, the use of wind turbines provides greater flexibility for implementing the RO membrane system in various locations around the world (Park et al.

2009). From many wind energy potential studies, world-wide wind resources are abundant (Ackermann and Söder 2002). For example, Matthies and Garrad found that offshore wind potential in Europe is around 2500 TWh/year which is about 85% of Europe's electricity consumption in 1997 (Ackermann and Söder 2002). Kalogirou in a review of renewable energy sources for desalination concluded that theoretically, the world's wind energy could supply an amount of electrical energy equal to the demand of electricity around the world (Goosen et al. 2011; Kalogirou 2005).World-wide wind capacity doubled about every three years during the last decade of the twentieth century. Table 2.3.2 shows the rapid increase of stand-alone wind generation capacity in Africa and the Middle East from 1995 to 2001. In order to adapt to the fast market development, wind turbine technology has experienced important evolution over time (Ackermann and Söder 2002). Modern wind turbines have improved significantly in their efficiency, reliability and power rating over last two decades and the wind electricity generation costs have fallen by 50% over last 15 years (Tzen 2009). The cost of wind electricity is very close to the power generated from conventional sources in some locations. Therefore, wind turbine technology is mature and commercially available (Subiela et al. 2009).

For communities on islands and insolated in land areas with abundant wind resources, wind power is even more competitive with conventional energy sources because electricity is usually expensive and unreliable (Forstmeier et al. 2007). Apart from that, wind energy requires less land area than the other renewable energies, which makes wind energy especially suitable for islands that have good wind energy and often

have very limited flat ground (Tzen and Morris 2003). It has been estimated that 1.4 x 10^{14} m^3 out of total 3.1x10^{14} m^3 saline groundwater in United States are co-located with sufficient wind resources for groundwater desalination (Androwski et al. 2011). In addition, compared with various other renewable energy resources, wind driven desalination has the least impact on the environment, which has an important environmental impact reduction of 75% (García-Rodríguez, L 2003; Ma and Lu 2011).

Table 2.3.2 Operational wind power capacity in the Middle East and Africa (Ackermann and Söder 2002)

Country, region	Installed capacity, MW		Increase over years, MW
	End 1995	End 2001	
Iran	1	11	10
Israel	6	8	2
Egypt	5	125	120
Morocco	0	54	54
Jordan	1	2	1
Rest of Africa	0	3	3
Total	13	203	190

There are typically two main types of wind energy usage for electricity generation: (1) the commercial generation of bulk electricity through grid-connected systems; (2) electricity generated within stand-alone systems (Miranda and Infield 2003).The major difference is that the second types of wind-electricity generation systems are built to be used in stand-alone sites where maintenance may be periodic and technical assistance limited, thus more effort is required in their design (Miranda and Infield 2003). Conventional power supply or grid connected turbines may be used as back-up if they are available. Sometimes, the wind can be the only source of energy and this should be taken into consideration during the design.

The nature of wind is one of the critical limiting factors to the wider implementation of wind driven desalination systems. There are two significant problems need to be solved: RO desalination technology is not suitable for operation under variable power input and the lack of continuity of energy supply may cause the fresh water demand not to be met (Miranda and Infield 2003). The use of batteries is a common solution to solve both problems; batteries accumulate energy (long-term storage) and smooth wind power variation (short term storage). The obvious downside is a significant increases in both capital and operating costs. Also, batteries require conversion of power from air motion to electricity, then another conversion from electricity to water pressure. Our study aims using a different kind of energy storage method, air pressure, where energy is converted once, from air motion to water (and air) pressure. This could result in lower energy losses and could be less expensive than batteries.

2.4. Existing Wind Powered RO Desalination Analysis and Prototypes

There are a number of existing papers focused on the feasibility, economic analysis, and novel configuration of wind powered RO desalination processes, which showed promise in dealing with variable flow and pressure operation of RO membranes.

2.4.1. Feasibility and economic analysis of wind powered RO processes

Feron (1985) evaluated the economic feasibility of a wind-powered RO plant by mathematical modeling and concluded that high wind speed and high fuel prices are the preconditions of economic wind powered RO (Charcosset 2009). His research also

indicated that wind-powered RO desalination could become more economical because of decreasing RO plant costs, the continuing development of membrane science, decreasing wind turbine costs, and steady or increasing fuel costs. The same result has also been demonstrated by Forstmeier et al. (2007).

Based on cost analysis on a wind-assisted RO system for desalinating brackish groundwater in Jordan conducted by Habali and Saleh, the cost for wind-powered brackish water desalination is projected to be less expensive than for a diesel powered system (Habali and Saleh 1994). The cost analysis was established from measured wind speed distribution and power curves of the wind-energy converter.

In an analytical study conducted by Kiranoudis et al. (1997), design parameter selections and different operational aspects are discussed for different wind turbines and membranes using both brackish water and seawater as feed water. They demonstrated that with at least 5 m/s average wind speed, the unit cost of freshwater production by a conventional RO plant can be reduced up to 20%. They also concluded that the fresh water production capacity was proportional to the size of the desalination units, but the capacity was not affected by either wind speed or wind turbine characteristics (Kiranoudis et al. 1997).

Garcia-Rodriguez et al. (2003) presented a preliminary cost evaluation of wind driven RO. They analyzed produced water cost based on climite conditions and plant capacity. The influence of possible changes in wind power and RO technologies on the produced water cost was also evaluated. They pointed out that wind-powered RO plants are competitive compared to conventional RO plants based on their cost analysis.

Karagiannis et al. (2008) found that for a stand-alone Wind-RO unit, the cost of produced freshwater can be as low as \$1.26 /m^3 for a medium-size installation, but it may reach \$6.29 /m^3 for small system. With electricity connection, the cost varies between \$1.76 /m^3 and \$2.74 /m^3 with low capacity, mainly around 1000 m^3. Even though the cost of using conventional RO is lower under some circumstances, the cost of using wind power is counterbalanced by the environmental benefits.

The cost analysis of desalination plants on Greek islands was conducted by Kaldellis et al.(2004) and it was found support for using a renewable energy-based desalination plants as the most promising and sustainable method to satisfy the fresh, potable water demands of the small- to medium-sized Greek islands at a minimal cost.

From the above literature it is apparent that wind power can greatly reduce the unit cost of RO desalination when properly designed. Therefore, wind-driven RO desalination is promising, especially considering the trends of continuing RO membrane development, decreasing turbine cost, and increasing fuel costs.

2.4.2. Existing Wind Powered RO Desalination Prototypes

Several wind-powered RO desalination prototypes have been successfully designed or implemented. Table 2.4.1 presents some of the most well-known Wind-RO plants around the world. They fall into two major classifications: system with or without an alternative electrical supply (grid or diesel generator).

Table 2.4.1 Wind energy driven reverse osmosis desalination plants (Tzen 2009)

Location	RO capacity, m^3/h	Electricity supply	Year of installation
Ile do Planier, France	0.5	SA[1]	1982
Island of Suderoog, Germany	0.25–0.37	SA	1983
Island of Helgoland, Germany	40	AES[2] (diesel)	1988
Fuerteventura, Spain	2.3	AES (diesel)	1995
Pozo Izquierdo, Gran Canaria, Spain	8 units ×1.0	SA	1995
Therasia Island, Greece	0.2	SA	1995/1996
Tenerife, Spain	2.5–4.5	SA and AES (grid)	1997/1998
Island of Syros, Greece	2.5–37.5	SA and AES (grid)	1998
Keratea, Greece	0.13	SA	2001/2002
Pozo Izquierdo, Gran Canaria, Spain	0.8	SA	2003/2004
Loughborough University, UK	0.5	SA	2001/2002
Milos island, Greece	2 × 41	AES (grid)	2007
Island of Irakleia, Greecea	3.3	SA	2007
University of Delft, Netherlands	0.2–0.4	SA	2007/2008

[1] SA – Stand-alone
[2] AES – Alternative electrical supply

2.4.2.1. Systems with back up (grid/diesel)

In these systems, the power input is maintained constant because of additional energy supplies, such as diesel generator and local grid. When wind power is not enough to provide RO operation energy, the back-up power will be used to make up the deficiency and maintain constant power supply. The significant advantage of this kind of

systems is that overall energy costs have been reduced and the fluctuation of power supply has been successfully avoided.

A wind-powered RO plant connected to the grid as auxiliary energy was installed at Los Moriscos (Gran Ganaria, Spain). The plant was designed to use brackish water as feed and had a capacity of 200 m^3 per day (García-Rodríguez 2003).

Another grid connected plant, the Kwinana Desalination plant, located to the south of Perth in Western Australia, has been successfully built and is operational (Dehmas et al. 2011). The plant supplies the Perth metropolitan area and can produce nearly 140 ml of drinking water per day. The 80MW Emu Downs Wind Farm generates the electricity for this plant (Dehmas et al. 2011).

A wind-driven seawater desalination plant with diesel as backup was built in 1993 at Fuerteventura Island, Spain (García-Rodríguez 2003). The plant has a capacity of 56 m^3 per day. The hybrid diesel-wind system consists of two diesel engines and a wind turbine of 225 kW which meets the energy requirement to produce drinking water for a village of 300 people.

The common thread among this type of RO system is that they do not operate when back-up power supply is not available, because in these systems, RO units cannot be driven solely by the wind turbine.

2.4.2.2. Systems without back up

Systems without back-up power sources are either operated in an approximately constant manner (using storage devices or on/off RO unit switching) or in variable power input conditions.

Approximately constant power input can be achieved by energy storage devices. Extra wind energy is accumulated in the storage devices when the power generated by the wind turbine is more than the demand of the RO unit. This stored energy will be used when wind power declines. Batteries and flywheels are the energy storage devices commonly used in stand-alone wind driven RO systems (Miranda and Infield 2003). A battery system is typically used for medium-term storage, while a flywheel is used for short-term storage (Folley et al. 2008).

A published stand-alone systems analysis dealt with the sensitivity of operation to wind speed, battery storage capacity and reverse osmosis operating pressure (Infield 1997). The conclusion was that it was economical to minimize the capacity of the battery store since water storage was much cheaper than electricity storage. The most effective battery capacity would be in the range of 4-8 hours at nominal rated load for a desalination plant, depending on the wind speed at the specific location. Design of a wind-driven RO with battery storage should carefully consider the relationship of feed pressure, battery size and actual wind speed, in order to reduce capital and maintenance costs as much as possible. But, the high cost of batteries and the possibility of available energy reduction still make this energy storage system economically unattractive (García-Rodríguez 2002).

Another prototype was constructed on the island of Gran Canaria in the Canarian Archipelago, which was a fully autonomous wind-powered desalination system (Carta et al. 2003). This system contained a wind farm, made up of two wind turbines and a fly wheel as energy storage mechanism for a group of eight RO modules and control subsystems. It was determined that both large and small scale seawater desalination could be achieved by this system in coastal areas with a scarcity of water and abundant wind resources.

Another option of maintaining near constant power input in wind-RO system is to use on/off RO unit switch. The wind-RO systems use several smaller RO units connected to higher power wind turbines. The units are turned on or off to match available power provided by wind turbine. This power control strategy largely reduced negative effects of wind fluctuation on RO operation and allows using high power turbines with hundreds of kilowatts.

Except for approximately constant power operation, variable power control strategy can also be applied in wind-RO system design. This strategy is based on certain RO operational limits which commonly are presented in RO operational window (Fig 2.1). When RO operation conditions (flow and pressure) lie within the RO operational window, the fixed automatic control is imposed no matter how wind is fluctuating. This control strategy allows less system operations and enables auto-operation over a wider range of power input without any energy storage devices or back-up. This control strategy largely reduced the capital, operation and maintenance costs. The drawback is

that it may reduce the membrane life time and effect RO performance because of variation operation.

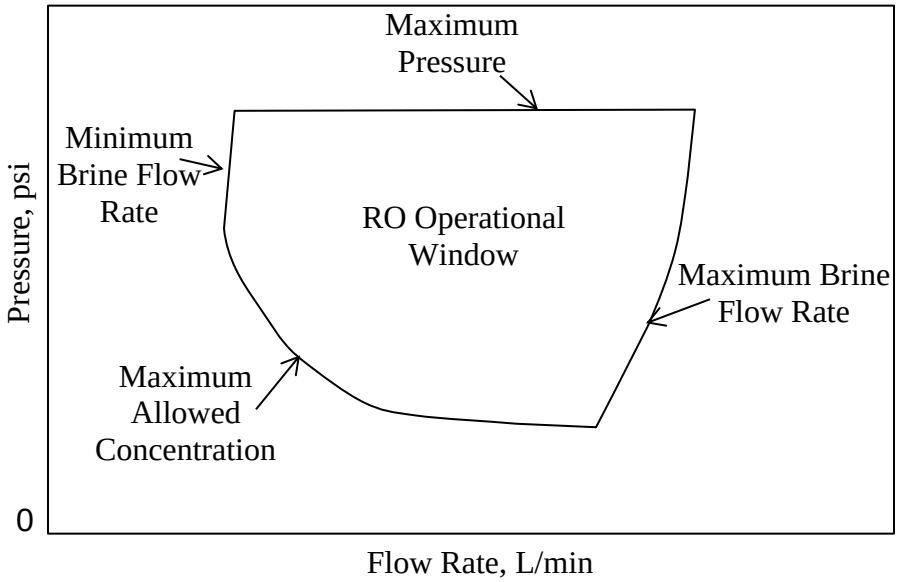

Figure 2.4.1 Example of RO Operational Window (Miranda and Infield 2003).

The variable-flow RO desalination unit developed by Miranda and Infield was driven by a 2.2 kW wind turbine generator (Miranda and Infield 2003). Variable flow operation allowed the system to accommodate with fluctuating and intermittent wind without energy storage and batteries. Water produced is dependent on the instantaneous wind speed.

Another wind-powered RO desalination system using variable power control was constructed and tested on Coconut Island off the northern coast of Oahu, Hawaii, for brackish water desalination (Gude et al. 2010; Habali and Saleh 1994; Liu et al. 2002). The system included four major subsystems, which were a multivaned windmill/pump, a flow/pressure stabilizer, an RO module, and a control mechanism. When the water

pressure dropped to 517 kPa because of diminishing wind, the control mechanism cut off the flow by closing the valve. Conversely, water pressure reached upper limit 724 kPa when wind picked up. The control sent a signal to relieve the valve to discharge the excess water from the system. The recovery ratio of 20% and average rejection of 97% were achieved with 3000 mg/l TDS and 13 l/min flow rate under 5m/s average wind speed. 35% Energy efficiency can be achieved with well-operated multi-vaned wind-mills.

This study focuses on a wind-powered RO desalination system combined with a compressed air energy storage system. This system was selected because (1) the energy storage device enables variable-speed and intermittent wind power to be effectively used, (2) it is cost-effective to use free wind power instead of electricity, especially for remote areas, and to store treated water using a storage tank instead of using battery to store electricity, (3) saltwater and winds are two natural resources that are often found together in coastal areas and small islands where this kind of technology might be viable.

CHAPTER 3 EXPERIMENTAL MATERIALS AND METHODS

3.1. Proposed Wind-RO System

The key difference between our proposed system and a traditional configuration is that the RO vessels will be pressurized by air to provide an energy buffer. This allows the RO element to be charged until sufficient energy is stored, and then desalination occurs using the stored energy. This design enables the use of fluctuating and intermittent wind power without an energy storage devices that is different from the batteries and flywheels that have been proposed previously. The energy is stored as pressured air, which is the kind of energy used for RO, so there are few energy transfer steps (as opposed to electrical or mechanical energy storage). These air-pressure-RO elements can be combined and tailored according to the capacity of wind turbine and expected wind pattern. Figure 3.1.1 shows several RO PVs coupling with a single wind turbine and the flow diagram of this design. This envisioned system can also be powered with electrical energy produced by multiple turbines.

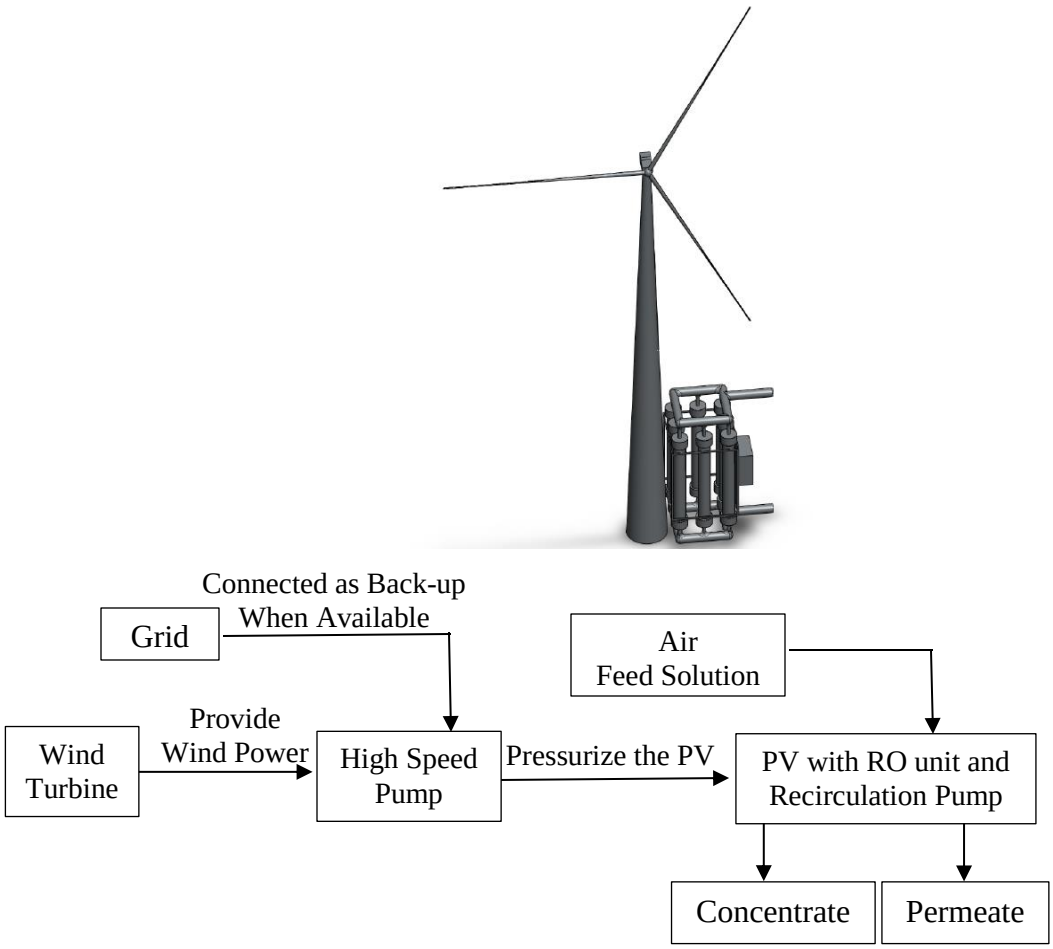

Figure 3.1.1 Conceptual drawing and process diagram of a wind-driven RO units connected directly to a turbine (The conceptual drawing was created by Pooja Mahajan).

In a conceptual sketch of a possible full-scale system configuration, the PVs are arranged vertically with one spiral-wound membrane module per PV (Figure 3.1.2). The membrane module will be at the bottom submerged in water and most of the vessel will be filled with salt water and high-pressure air. A small immersible recirculation pump will be placed in the PV to achieve crossflow. A high-speed pump will connect to the wind turbine directly to pump in feed solution, while the small recirculation pump will be driven by either the turbine or grid electricity.

One way that the system could operate is under "batch mode." Batch mode desalination could use three steps per run: 1) fill the vessel partially with saltwater (the vessel is initially charged with compressed air), 2) desalinate water by releasing permeate with the cross flow pump running, and 3) discharge the concentrated saltwater left in the vessel after desalination.

Another operation mode is the "steady-state" condition. Under steady-state mode, saltwater is recycled by the high speed pump to keep nearly constant pressure in the vessel and provide crossflow, while permeate is released over time. Under this mode the recirculation pump will be used only when wind energy is not high enough to drive the high-speed pump to provide both pressurizing and crossflow. In other words, batch mode will be applied when wind energy is relatively low and time is required to fill the PV. Steady-state mode would be used when wind energy is high enough to operate the RO system continuously.

This unique design is ideal for variable wind energy due to the fact that the pressurization and desalination process can be started at any time as long as wind is available. If the wind dies, the PV remains pressurized at its current level and the system simply waits until wind picks up to continue desalination when salt rejection dropped too much. While the wind speed is low, there is no energy loss because the energy stores in the PV and the system remains pressurized until enough wind power is available. The clean water produced can be easily stored so there is no demand-side driver for constant water production. In order to test whether our full-scale conceptual idea would be

feasible, we have planned several sets of bench-scale experiments, as described in the flowing experimental methods section.

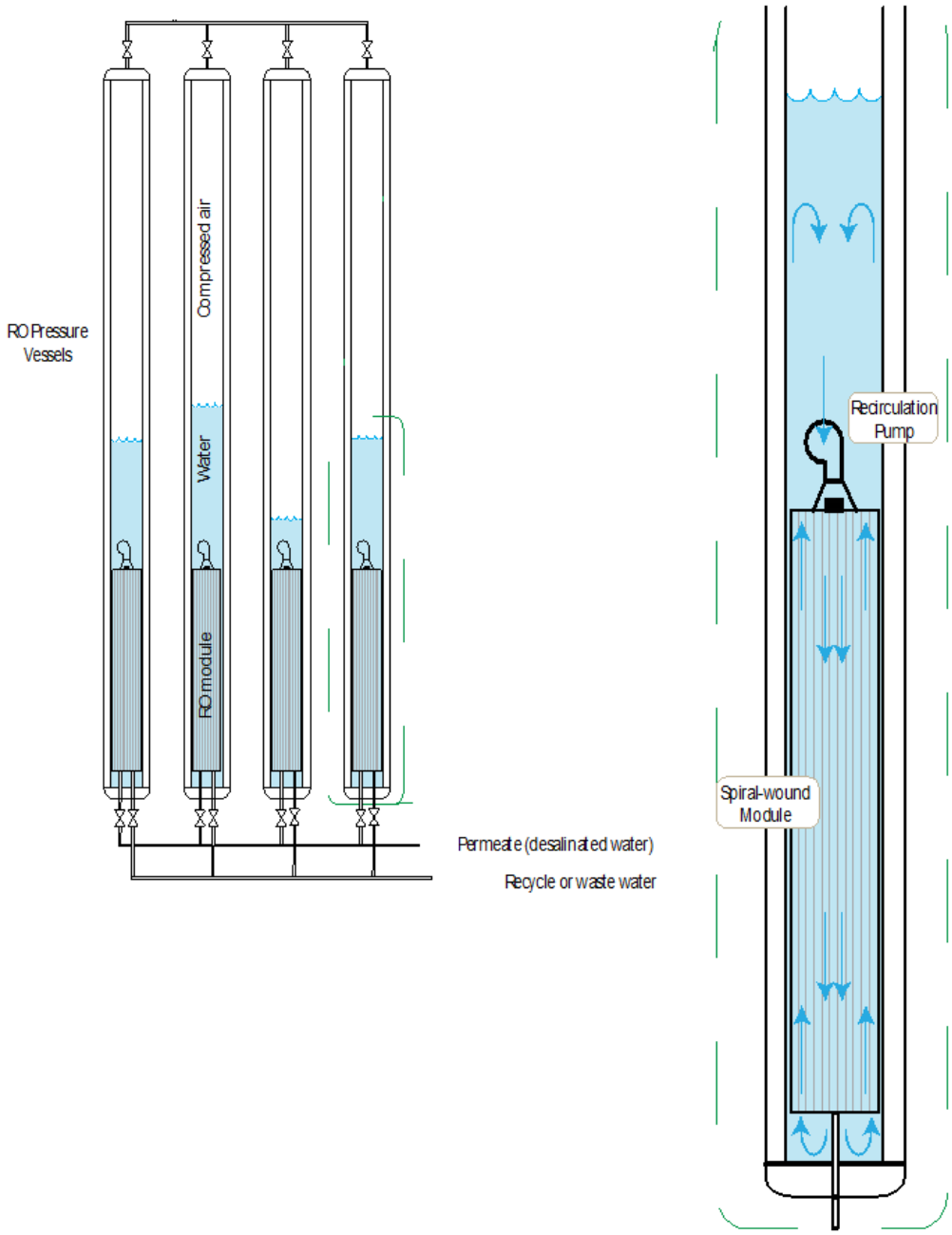

Figure 3.1.2 Conceptual sketch of a direct-driven full-scale wind-driven RO desalination system.

3.2. Laboratory Wind-RO System Set-up

The bench-scale air-driven RO system is built by modifying a bench scale setup already available in the laboratory. Figure 3.2.1 shows the already-available system. The key components were the membrane test cell (SEPA II, GE Osmonics, Minnetonka, MN), positive displacement pump, motor, pressure gauges, temperature control unit, conductivity probes, valves, balance and data acquisition system. Stainless-steel tubing and compression fittings were used to connect all the components. Other detailed information about the previous bench-scale system is provided elsewhere (Ladner 2009).

In the modified bench scale system with energy storage device, a 10.7 L PV was installed between the high-speed pump and the membrane cell. The PV was built by welding stainless steel caps onto a stainless-steel pipe. It can successfully withstand over 1000 psi pressure. In order to be able to bypass the PV, new tubing and ball valves were installed. A compressed nitrogen cylinder (nitrogen tank) was connected to the PV for pre-charging (Figure 3.2.2). A regulator with 0-800 psi range was connected to the nitrogen tank to allow different initial gas pressure in the PV. An automatic needle valve (actuator) was installed in the concentrate line after the membrane cell to enable automatic pressure control, even as the pump speed was varied to simulate different wind patterns. Permeate flowed into a centrifuge tube with a piece of plastic tubing sticking to its bottom. This device was used to hold small amount of permeate and enabled insertion of a conductivity probe to measure inline permeate conductivity. The permeate water flowed from the tube into a flask placed on a balance to measure the accumulated mass of the permeate. Specifications for all the components are listed in Table 3.2.1.

LabVIEW 7.0 is a system design software that we used for data acquisition, interpretation and experiment control. The LabVIEW program automatically recorded and monitored feed conductivity, permeate conductivity, salt rejection, applied pressure, actuator (pressure control device) voltage and fluxes, while temperature and volume of feed solution in the feed tank were manually entered on the LabVIEW interface. An interval of 10 seconds was applied in the LabVIEW program and the data were recorded as the average of 100 data points. The actuator was also controlled by LabVIEW to maintain the target pressure in the event of pressure spikes. A target pressure was entered on the interface and the actuator was adjusted by the difference between and average pressure in each interval.

Automated pump speed control was implemented to enable simulation of fluctuating wind power input. Detailed information of this modified LabVIEW program is provided in section 3.5.4.

Data were recorded by LabVIEW with a unique filename and stored in a specific folder, which allowed the file to be recognized by MATLAB programs (see Appendix C). Also, the experimental data can be extracted and analyzed using these programs. Figures presented in this thesis were also generated using MATLAB software.

Table 3.2.1 Components of the bench-scale air-driven RO set-up. Modified from Ladner (2009).

Description	Manufacturer/Vendor	Model/Catalog #
Membrane test cell	GE Osmonics, Minnetonka, MN	SEPA II
Pump Cat Pumps,	Minneapolis, MN	231
Motor	Marathon Electric, Wausau, WI	MicroMAX 145THFR5329/Y368
Phase inverter	Toshiba, New York , NY	S-11
Pressure transducer (Pf)	Cole Parmer, Vernon Hills, IL	68072-14
Nitrogen tank	Clemson Workshop	N/A
Regulator	McMaster-Carr	3950T212
Actuator	Hanbay Laboratory Automation	MCJ-000AB-3-SS-2MG4
Stainless steel tubing	Swagelok, Solon, OH	SS-T6-S-035-20
Elbows, Ts, Couples	Swagelok, Solon, OH	SS-600 series
Regulating needle valve	Swagelok, Solon, OH	SS-1RS6
Ball valves	McMaster-Carr	46495K18
Pressure relief valve	Swagelok, Solon, OH	SS-4R3A5; spring kit 177-R3A-K1-C
Permeate flow meter	Alicat Scientific, Tucson, AZ	L-10CCM-D
Conductivity probes	Sensorex	CON500, CS150TC-PT1-6'-TL, FC50P
Balance	Mettler Toledo, Columbus, OH	PB3002-S
Temperature controller	Cole Parmer, Vernon Hills, IL	EW-12101-00
Data acquisition card	National Instruments, Austin, TX	PCI 6024E
Shielded I/O Connector Block	National Instruments, Austin, TX	SCB-68
Programming software	National Instruments, Austin, TX	LabView 7.0

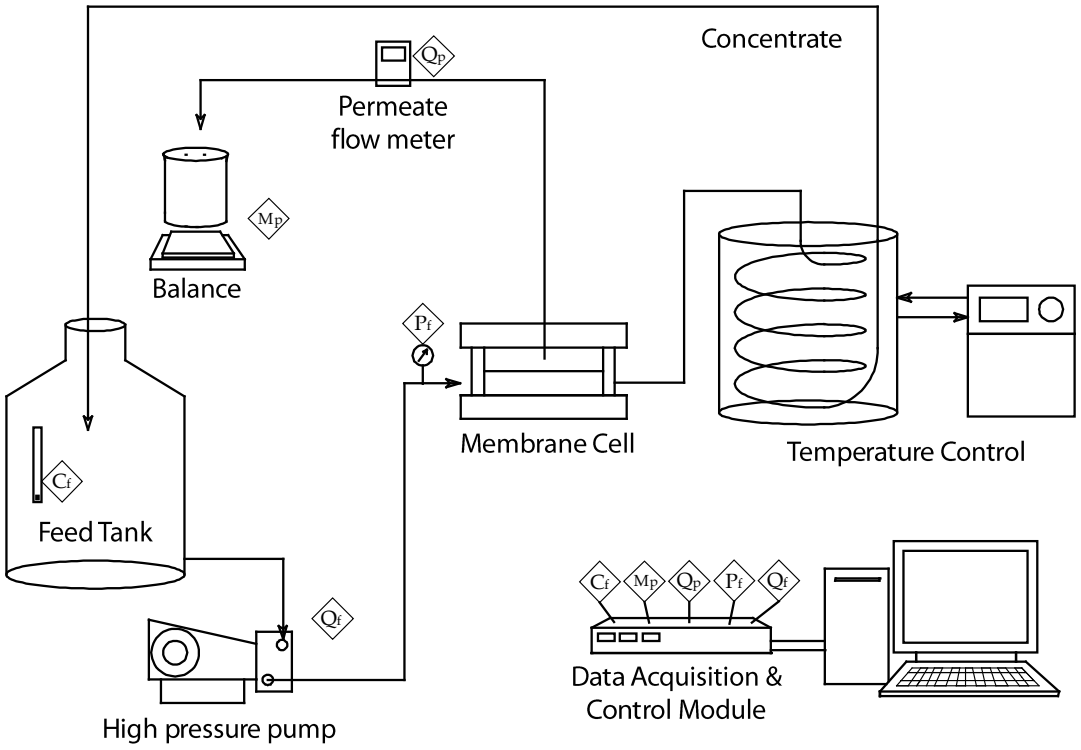

Figure 3.2.1 Diagram of the previously-available bench-scale RO membrane testing unit. symbols indicate electronic interface between the computer and components. Automated data acquisition locations are shown for feed conductivity (Cf), feed pressure (Pf), permeate flow rate (Qp), and permeate mass (Mp). Automated control of the high-pressure pump, and thereby the feed flow rate (Qf), is also indicated.

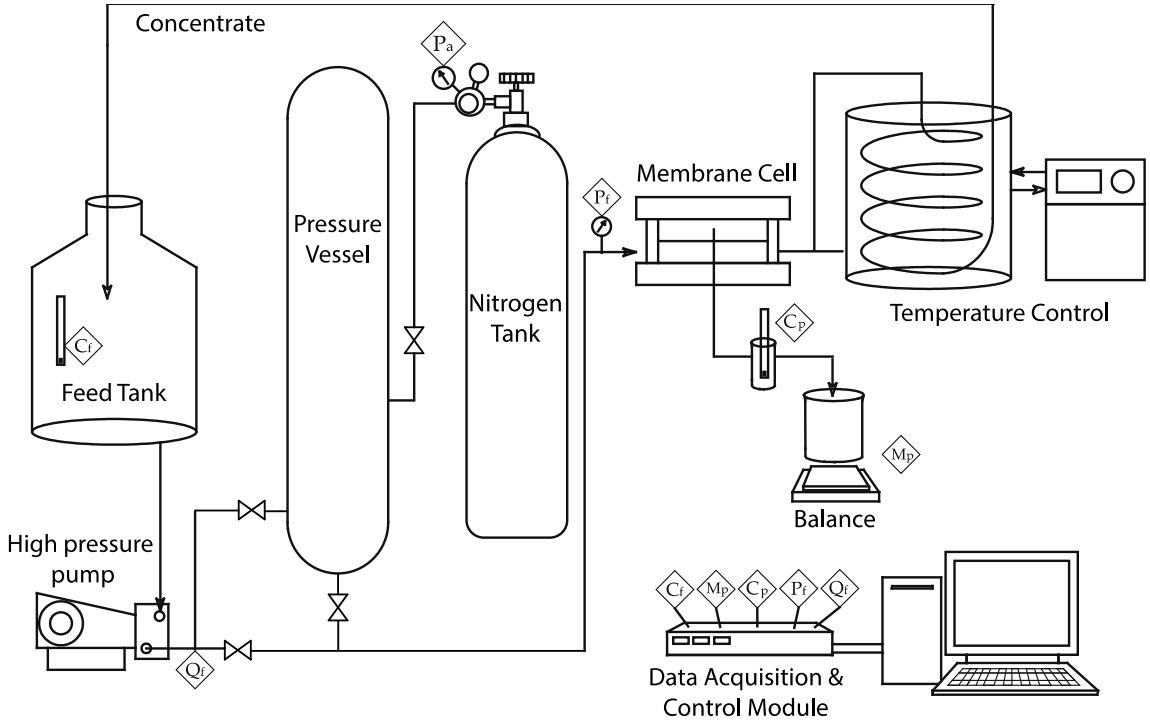

Figure 3.2.2 Modified bench-scale RO system with air-driven operation. Compressed air is connected to the PV and the pressure (Pa) is monitored. The high-pressure pump is driven by a motor and the flow rate (Qf) is controlled. Desalinated water is fed to the balance, and the mass (Mp) is recorded over time to calculate flux. RO feed pressure (Pf), feed conductivity (Cf) and permeate conductivity (Cp) are also monitored. The SCADA system records all data and controls the feed recirculation rate.

3.3. Water Quality and Analysis

The feed solution was prepared by mixing deionized (DI) water and molecular biology grade sodium chloride. The concentrations used in the experiments were 0, 15, 25 and 35 g/L. 14 L of fresh salt water were prepared for each experiment on the day before and 2 L were wasted to flush DI water out of the experimental system every run. The concentrate was recycled back to the feed tank in all the experiments. The conductivity of the feed and permeate were measured using conductivity probes.

3.4. Membrane

The RO membrane used in the experiments was catalog number SW30HR from Filmtec, a wholly owned subsidiary of the Dow Chemical Company (Midland, Michigan). Membranes were received as flat sheets and were stored dry in sealed plastic bags protected from light. Membrane coupons were cut to 14.6 cm by 9.5 cm and stored in DI water at 4 ˚C the night before experiment. Since no fouling was observed in the experiments, a single membrane coupon was used for each set of experiments, constituting several runs with varying operating parameters over several days.

3.5. Experimental Methods

Unlike the proposed Wind-RO system where two pumps are envisioned (a high-pressure pump feeding the system and a crossflow pump inside the PV), the pump in the experimental setup is placed outside the PV and used to provide both high pressure and crossflow. The pump can be operated with a wide range of pressures and flow rates, from 1 cm/sec to 90 cm/sec crossflow velocity and 700 to 1000 psi pressure, which

allows flexibility in the experimental design. The experiments were conducted to test effects of dissolved air, and performance under steady state mode, batch mode, controlled power fluctuation and controlled power intermittency. The experimental details for each of these situations is presented in the following four sections.

3.5.1. Dissolved Air Effects

One potential problem in the proposed system is that air may dissolve into water under high pressure in the PV. The dissolved air may affect the RO membrane performance. Three sets of experiments were conducted to determine the effects of dissolved air, if any. Crossflow velocity was set at 47 cm/sec for all the experiments in this section.

The amount of air dissolved into water in the PV was determined by conducting a 4 hour steady-state experiment under 1000 psi. The PV was pre-charged with 400 psi air pressure. The feed solution was 35 g/L NaCl solution and the volume was 14 L with 2 L wasted to flush out DI water in the laboratory system. The volume of feed solution (V_f) left in the feed tank was entered manually into the LabVIEW program every 5 mins. The volume of salt water (V_{sw}) and air (V_{air}) in the PV were calculated by the following equations:

$$V_{sw} = V_i - V_f \quad [2]$$

$$V_{air} = V_{pv} - V_{sw} \quad [3]$$

Here V_i is the volume of initial feed solution used for this experiment (12L) and V_{pv} is the volume of the PV (10.7 L). All the parameters in the above equations are in units of liters.

The effects of different air:water ratios were tested by changing the initial mass (pressure) of air in the PV. The initial charged air pressures were 0, 200, 400, and 600 psi respectively. Steady-state experiments were run at 1000 psi. 35 g/L NaCl solutions were used as feed in these experiments.

Comparison experiments in two different modes, conventional RO steady state without energy storage and wind RO steady state with energy storage were also conducted to further understand the effects of air on RO membrane performance. The experiments were carried out using 0, 15, 25, and 35g/L NaCl feed solution under both modes for two hours 1000 psi steady state. 400 psi initial air pressure was applied in wind RO steady state experiments.

3.5.2. Operational Characteristics under Steady State Mode

Operational characteristics under steady state with energy storage were determined by changing one experimental parameter at a time. All the experiments conducted in this section used constant 1000 psi pressure.

Different concentrations of feed solution were tested to determine the possibility of treating both brackish water (15 g/l and 25 g/l NaCl) and seawater (35 g/l NaCl). Steady-state experiments lasted two hours. The crossflow velocity was 47 cm/sec and the initial air pressure was 400 psi for this series of experiments.

Experiments were also performed with three crossflow velocities (32 cm/sec, 47 cm/sec, 61 cm/sec) under steady-state conditions with the PV. The feed solution concentration used was 35 g/L and the initial air pressure was 400 psi.

3.5.3. Operational Characteristics under Batch Mode

Batch mode experiments began at 1000 psi after a two-hour steady-state run to mimic the second step of the proposed Wind-RO system, which was desalinating water by releasing permeate without pumping in feed.

Batch mode experiments without cossflow were conducted first to serve as a baseline for experiments with crossflow. By isolating the PV from the rest of the Wind-RO set-up, the pressure remaining in the PV drove the desalination process. As permeate was released, the pressure in the PV decreased. Feed solution with 35 g/L salt concentration and 400 psi initial air pressure were used. The experiments lasted 4 hours.

The other set of batch mode experiments used the high speed pump to provide crossflow. Different feed concentration (15, 25, and 35g/l NaCl) experiments were conducted using 47 cm/sec crossflow velocity and 400 psi initial air pressure. Experiments were also performed at 3 crossflow velocities (32, 47, and 61 cm/sec) using 35 g/L feed concentration and 400 psi initial air pressure. Finally, batch mode with crossflow was tested with different initial air pressures of 0, 200, 400, and 600 psi.

A theoretical relationship between pressure in the PV and permeate mass was developed for batch mode experiments with crossflow using the following equation based on the ideal gas law.

$$M_p = \rho_f P_s V_{air} (1/P_b - 1/P_s) \quad [4]$$

Where M_p is accumulated permeate mass (g), ρ_f is feed density (1035 g/L), P_s is steady-state applied pressure (1000 psi), V_{air} is volume of air in the PV, P_b is the batch

mode pressure in the PV. V_{air} was 0.96, 1.78, 2.68, and 5.53 L, respectively with 0, 200, 400, and 600 psi pre-charged air pressure after 2 hours steady state operation.

The theoretical relationship of pressure in the PV versus permeate mass under batch mode with crossflow was plotted in figure 3.5.1. The balance was tared at the beginning of each batch mode experiment. The applied pressure was adjusted by manually changing the actuator voltage on the LabVIEW interface according to the theoretical relationship and accumulated permeate mass.

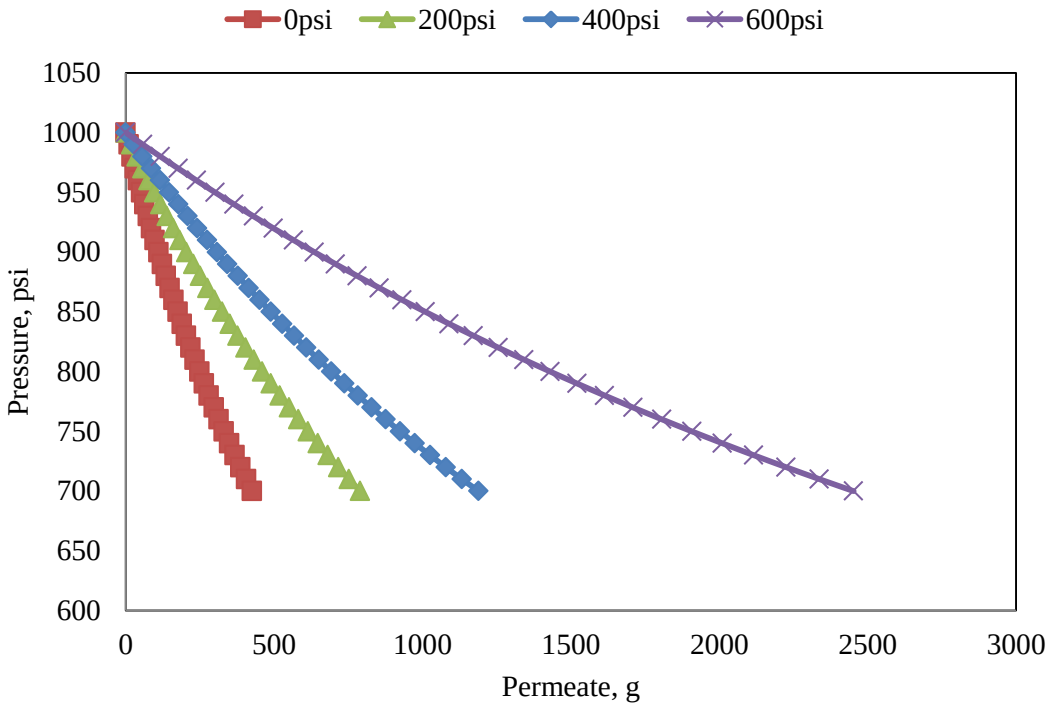

Figure 3.5.1 Theoretical pressure in the PV and permeate released from the vessel during batch mode experiments with crossflow under different initial air pressures. Permeate released from the vessel is calculated using the ideal gas law assuming that the air will not further dissolve into the water during batch mode experiment.

3.5.4. Controlled Fluctuations

Sinusoidal oscillations were used to simulate fluctuating wind speeds in order to simplify practical experiments (Lising and Alward 1972) and perform theoretical analysis (Rosen and Sheinman 1996). The pump speed control in LabVIEW was reprogrammed to enable fluctuating pump speed which mimicked wind power fluctuation. The experiments were run at steady-state with 8.0 Hz pump speed for a half hour and then switched to fluctuating mode. Steady state pump speed was used as average pump speed in fluctuating mode. Cosine waves started from the average value, while sin waves started from the maximum value. Therefore, in the experiments presented in this thesis, sinusoidal oscillations were changed to cosine waves to avoid sudden jumps from average pump speed to maximum pump speed. The wind speed v(t) at a certain time t is then defined as,

$$v(t) = U + A\cos\left(2\pi\frac{t}{T}\right) \qquad [5]$$

Where U is the non-zero center amplitude, A is the amplitude of fluctuation and T is the period of oscillation.

The pump speed was controlled in Labview to vary in a cosine pattern similar to Figure 3.5.2 A. The maximum (8.0 Hz), minimum (4.8 Hz) pump speeds and period were enterned on the LabVIEW interface before the fluctuating mode started. The average pump speed was set at 6.4 Hz, the peak to peak amplitude was set at 1.6 Hz, and 35 g/L salt solution was used for all the experiments in this section. Three sets of experiments were designed to demonstrate the effectiveness of this Wind-RO configuration to handle fluctuating wind conditions.

In the first set of experiments, the actuator was disabled, and its position remained constant as the pump speed fluctuated. The experiments were run at steady state for 30mins followed by 2 hours of fluctuating mode operation. In this set of experiments, the period of cosine wave was set at 5 mins. The experiment bypassing the PV was run as control, while experiments with different initial air pressures, 0, 200, 400, and 600 psi, were conducted.

The second set of experiments were designed the same as the first set, except that the actuator was enabled under fluctuating mode to try to maintain a target pressure. The target pressure was set at 950 psi instead of 1000 psi to prevent pressure overshooting. The actuator control portion in LabVIEW was reprogrammed in order to let the actuator react much quicker to keep the target pressure according to the difference between actual pressure and target pressure. The loops in previous LabVIEW program ran every 10 sec and 100 data points were captured in 10 sec. The average of these 100 data points was used to compare with target value and to control the process. After reprograming, the actuator control was enabled to send out a signal every 1 sec which was average of 10 data points, allowing for faster control. The rest of the LabVIEW program remained the same as the previous version. This new feature allowed the actuator to adjust and affect the pressure much faster to keep up with the highly fluctuating pump speed.

The period of oscillation was also varied during experiments. An initial air pressure of 400 psi was used in this set of experiments. The actuator was also enabled with a target pressure of 950 psi. Four different periods were 2.5, 5, 7.5 and 10 mins.

3.5.5. Controlled Intermittency

The performance of this system with air pressure as an energy storage buffer was further tested by simulating intermittent wind power similar to Figure 3.5.2.B. Seawater (35 g/l NaCl) was used as feed and initial air pressure was 400 psi for all the experiments in this section.

Intermittent operation was simulated by turning the pump off for a certain length of time and starting the pump up. The experiments were run at 1000 psi steady state for 30mins. The pump speed was 6.4 Hz and the period of no power was set at 5 mins. Sufficient time was given for the system parameters to return to their original values after the period of no power. The experiments were conducted under four scenarios:

1) Conventional RO without crossflow during wind off time: in this scenario, the actuator was fully open and pressure was totally released. The pump was stopped and no crossflow was provided. After 5 mins, the pump was restarted at 6.4 Hz and then the actuator was quickly closed by entering a certain voltage on the LabVIEW interface to achieve 1000 psi pressure.
2) Conventional RO with crossflow during the wind off time: in this scenario, pressure was released by fully opening the actuator with the pump running at 6.4 Hz all the time. After 5 mins, the actuator was closed to get 1000 psi pressure in the system.
3) Wind-RO without crossflow during the wind off time: in this scenario the PV was bypassed during the wind off time. The pressure built in the PV was used to produce permeate. After 5 mins, the PV was reconnected with the pump.

4) Wind-RO with crossflow during wind off time: in this scenario, the pump was only used to provide crossflow, but not pumping extra feed solution to maintain the pressure in the PV during wind off time. After 5 mins, the system went back to steady state mode, in which the pump provided crossflow and maintained 1000 psi pressure in the PV.

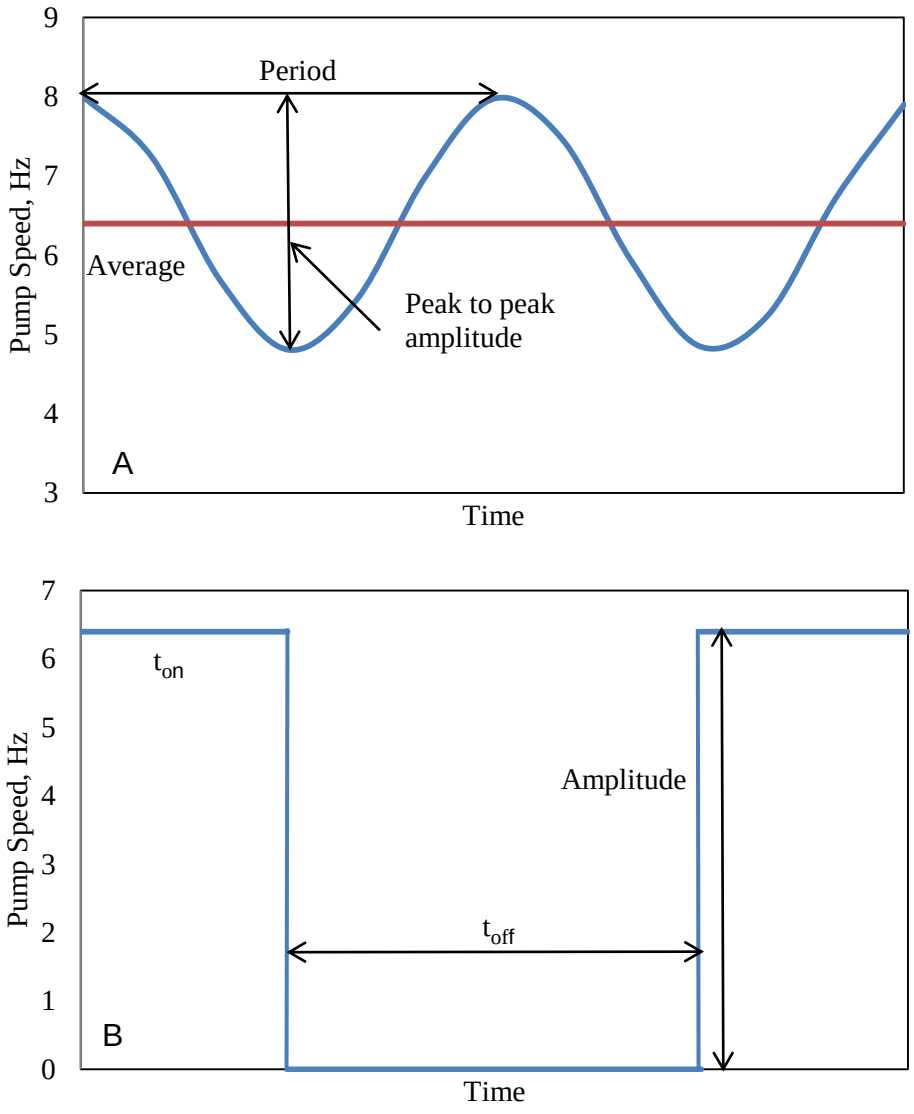

Figure 3.5.2 *(A) Sinusoidal pump operation; and (B) intermittent pump operation.*

CHAPTER 4 RESULTS AND DISCUSSION

4.1. Effects of Dissolved Air on the Performance of the Wind-RO System

Air dissolving into the feed water in the PV under high pressure may influence the performance of the membrane in a Wind-RO system. Three sets of experiments were conducted to evaluate the amount of dissolved air in the feed salt solution and to determine its effects.

4.1.1. Amount of Air Dissolved into Water Over Time

A four-hour experiment was conducted to calculate how much air dissolved into the water in the PV under 1000 psi. The PV was pre-pressurized by nitrogen to 400 psi. The salt concentration of feed solution was 35 g/L. The volume of feed solution (V_f) left in the feed tank was recorded manually in the LabVIEW program every 5 mins. The volume of salt water (V_{sw}) and air (V_{air}) in the PV were calculated using equation [2] and [3], respectively. The data over four hours were plotted in Figure 4.1.1.

The results indicated that nitrogen dissolved into the feed solution gradually. After 4 hours, the volume of nitrogen in the PV (V_N) reduced by 0.26 L over four hours. The total salt water volume (V_i) in the experimental system was 12 L. The nitrogen concentration in the PV was calculated using following equation,

$$C_N = fV_N \rho_N / V_i \qquad [6]$$

Where C_N is nitrogen concentration in salt water, f is the nitrogen loss percentage and ρ_N is density of nitrogen. ρ_N is 1.165 kg/m^3 under normal temperature and pressure (20^{o}C and 14.7psi). ρ_N under 20^{o}C and 1000 psi was calculated by following equation.

$$\rho_{N2} = \rho_{N1}(P_2T_1/P_1T_2) \qquad [7]$$

Therefore, ρ_N was 79.25 kg/m^3 in the PV head space. There was some nitrogen loss because the salt water recycled back to feed tank was under atmospheric pressure and nitrogen solubility decreased dramatically. A total of 50% nitrogen loss in 0.26 L nitrogen reduction was assumed, because salt water was exposed to the atmosphere about 50% of time and dissolved nitrogen was released to the atmosphere. The nitrogen concentration in the salt water was 0.86 g/L calculated from Equation 9. The theoretical amount of nitrogen dissolved was calculated using Herry's Law,

$$C_N = p_g / k_H \quad [8]$$

Where C_N is the solubility of dissolved gas, k_H is proportionality constant depending on the nature of the gas and the solvent, and p_g is partial pressure of the gas.

In this case, k_H was 1600 atm/(mol/liter) and p_g was 1000 psi. The theoretical amount of nitrogen dissolved in water was 1.19 g/L. The experimental nitrogen concentration in the salt water was less than the theoretical amount of nitrogen, therefore, under 400 psi initial gas pressure, nitrogen did not reach saturation in the 35 g/L salt solution. With increasing initial gas pressure, there is potential of further increasing nitrogen concentration in saltwater.

The effects of dissolved nitrogen in water were determined in the following two sections.

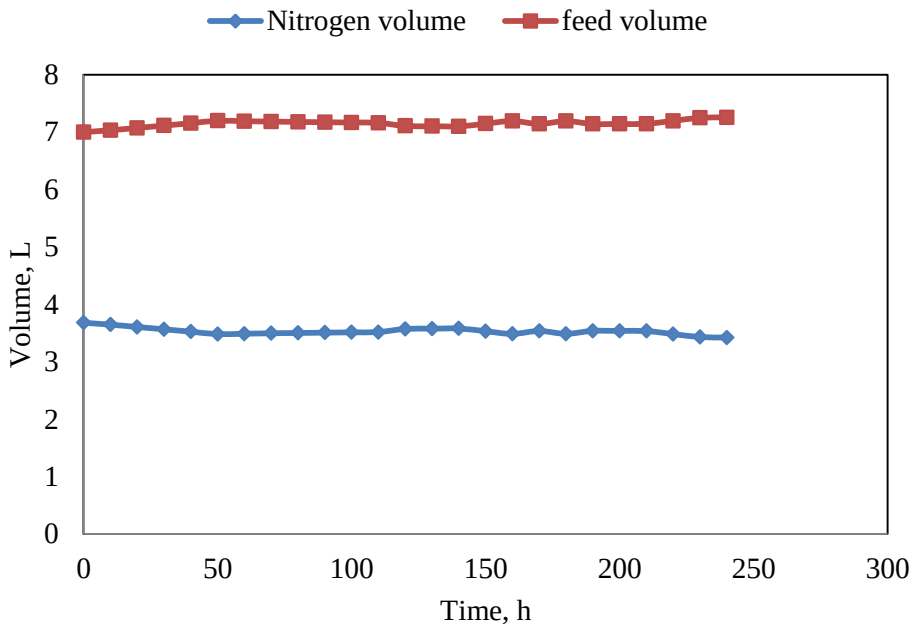

Figure 4.1.1 Nitrogen volume (blue) and salt solution volume change (red) in the PV with 400 psi initial air pressure at 1000 psi steady state.

4.1.2. Different Air:Water Ratio Effects

The different air:water ratio influence on the RO desalination process under steady-state and batch modes are shown and discussed in section 4.2.3 and 4.3.2.3 respectively.

4.1.3. Wind-RO and Conventional RO Performance Comparison

Experiments were performed to compare the steady-state performance of the conventional RO without PV and wind RO with PV. The experiments were carried out using 0, 15, 25, 35 and 45 g/L NaCl feed solution under both conventional RO and wind RO 1000 psi steady state. The PV was pre-charged with nitrogen to 400 psi for all wind RO experiments.

Fluxes were evaluated to determine the performance with and without PV. From Figure 4.1.2.A, the flux of wind RO was higher than conventional RO with feed concentration of 0 and 35g/L. For feed concentration of 15, 25, and 45g/L, the flux of conventional RO was higher than the flux of wind RO. Average fluxes under the two modes using different feed concentrations are presented in Figure 4.1.2.B to better see the trend. The conclusion is that the RO process with PV did not show a consistent benefit or detriment in flux compared to the conventional RO process.

In Figure 4.1.3, the average salt rejection under the two modes using different feed concentration is presented. Wind RO always had a higher rejection than conventional RO over the range of feed concentration tested in the experiments. The rejection of wind RO decreased with increasing feed concentration, while rejection of conventional RO did not follow any pattern. With all four different feed concentrations,

the wind RO process showed a slight advantage over the conventional RO process from the aspect of rejection improvement. However, the conventional RO experiments were conducted using different RO membrane coupons, which usually caused rejection variation under the same operation conditions. Hence, duplicate conventional RO experiments are needed to further prove the conclusion.

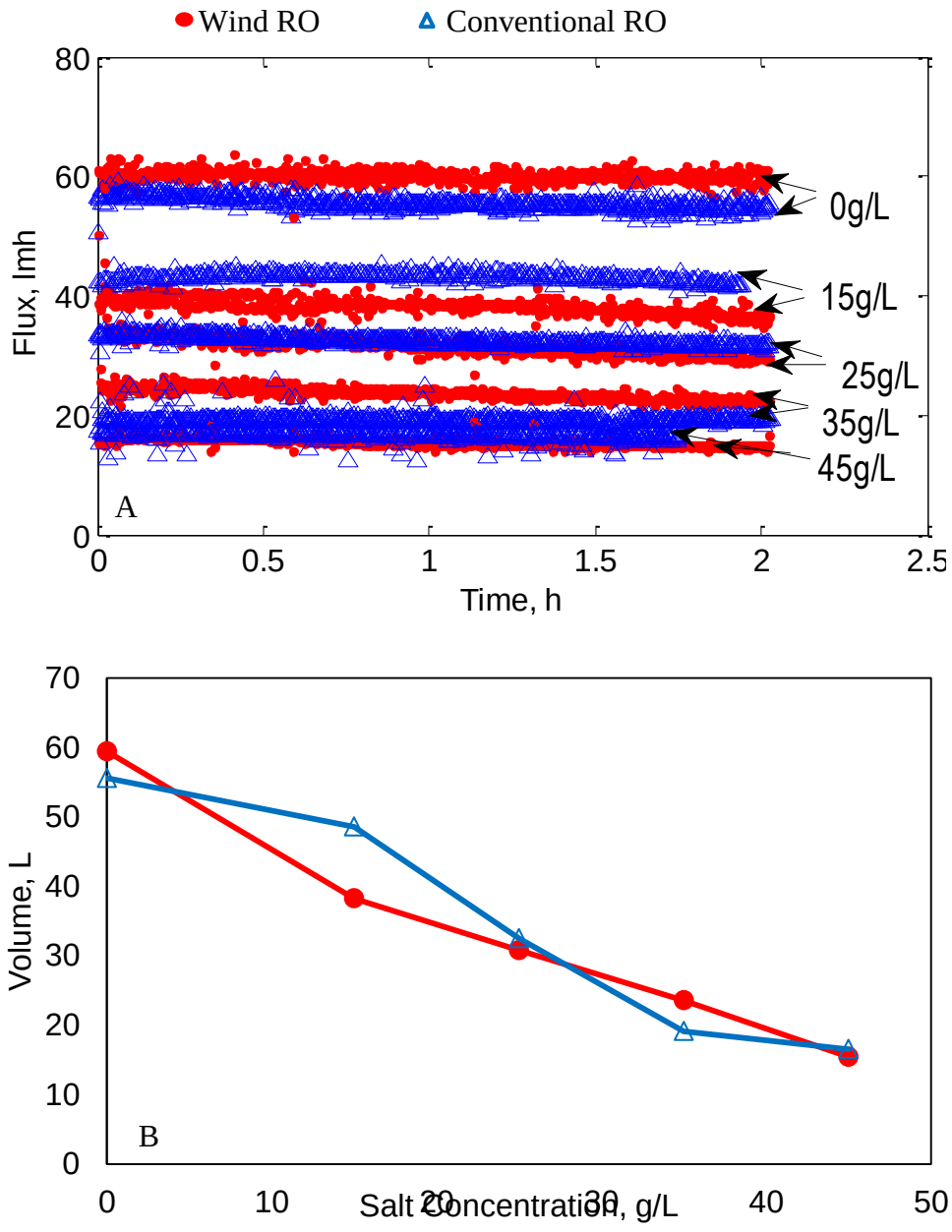

Figure 4.1.2 (A) Steady-state fluxes under wind driven RO mode and conventional RO mode. (B) Average steady-state fluxes under wind driven RO mode and conventional RO mode

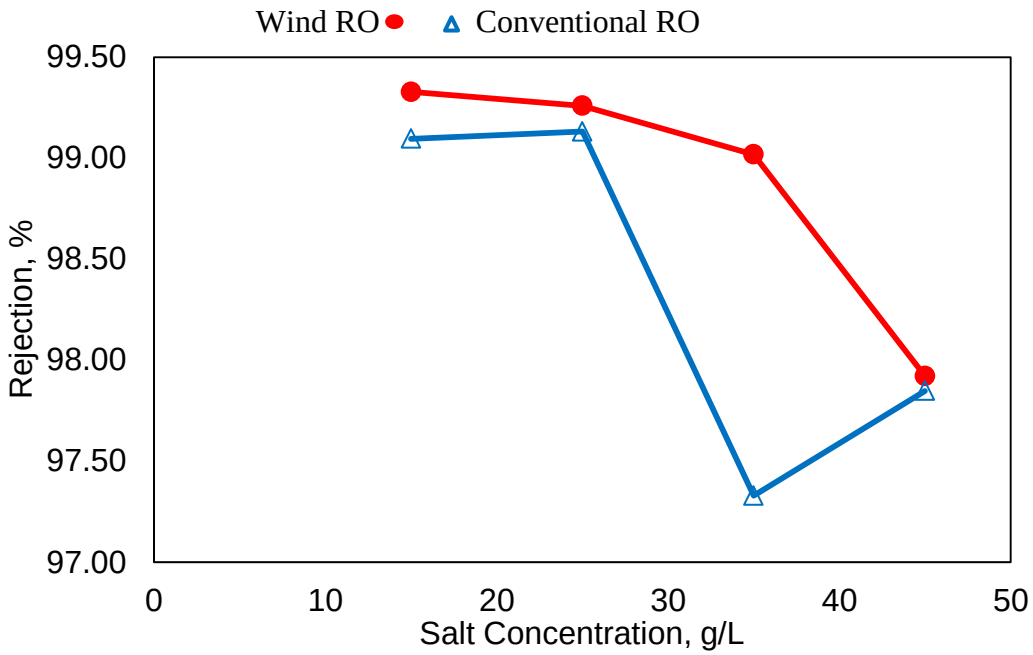

Figure 4.1.3 Average steady state salt rejection under wind driven RO mode and conventional RO mode

4.2. Wind RO Operation Characteristics under Steady-State Condition

The steady-state experiments served as a baseline for batch mode, intermittent power and fluctuating power experiments. Steady-state operation characteristics with energy storage were determined by conducting experiments under different feed concentrations, crossflow velocities and air:water ratios. All the experiments in this section were under constant 1000 psi pressure and run at steady state.

4.2.1. Steady State Operation Characteristics Using Different Feed Concentrations

A wide range of feed concentrations (15, 25, 35, and 45 g/L) were tested to determine the possibility of treating both brackish water and seawater. Two-hour steady state experiments with the PV were maintained at constant 1000 psi as shown in Figure 4.2.1 (A). The crossflow velocity was 47 cm/sec and the initial air pressure was 400 psi for this series of experiments.

From Figure 4.2.1.B, flux decreased as feed NaCl concentration increased. The reason is that high feed NaCl concentration induced high osmotic pressure which increased the resistance to the solvent flow and thus reduced the permeate flux. The fluxes decreased through the two-hour experiment because the permeate was wasted and the feed concentration increased.

In Fig. 4.2.1 (C) the feed NaCl concentration increased continuously over 2 hours, due to the fact that concentrate was recycled back to the feed tank after desalination and the permeate was wasted. From Fig. 4.2.1 (D), the permeate NaCl concentration decreased at the beginning of the experiments and stabilized after steady-state condition

was achieved. It was observed that high feed concentration resulted in relatively high NaCl concentration in the permeate.

From Fig. 4.2.1 (E), rejection also followed the same trend as fluxes. As salt concentration increased, osmotic pressure increased. The increasing osmotic pressure offset the feedwater driving pressure, resulting in flux decline. Increase in salt passage through the membrane (decrease in rejection) occurred as the water flux declined.

Expected results were achieved by wind-driven steady state experiments with different feed concentrations. It demonstrated that wind-driven RO desalination with energy storage device is suitable to treat both brackish water and seawater.

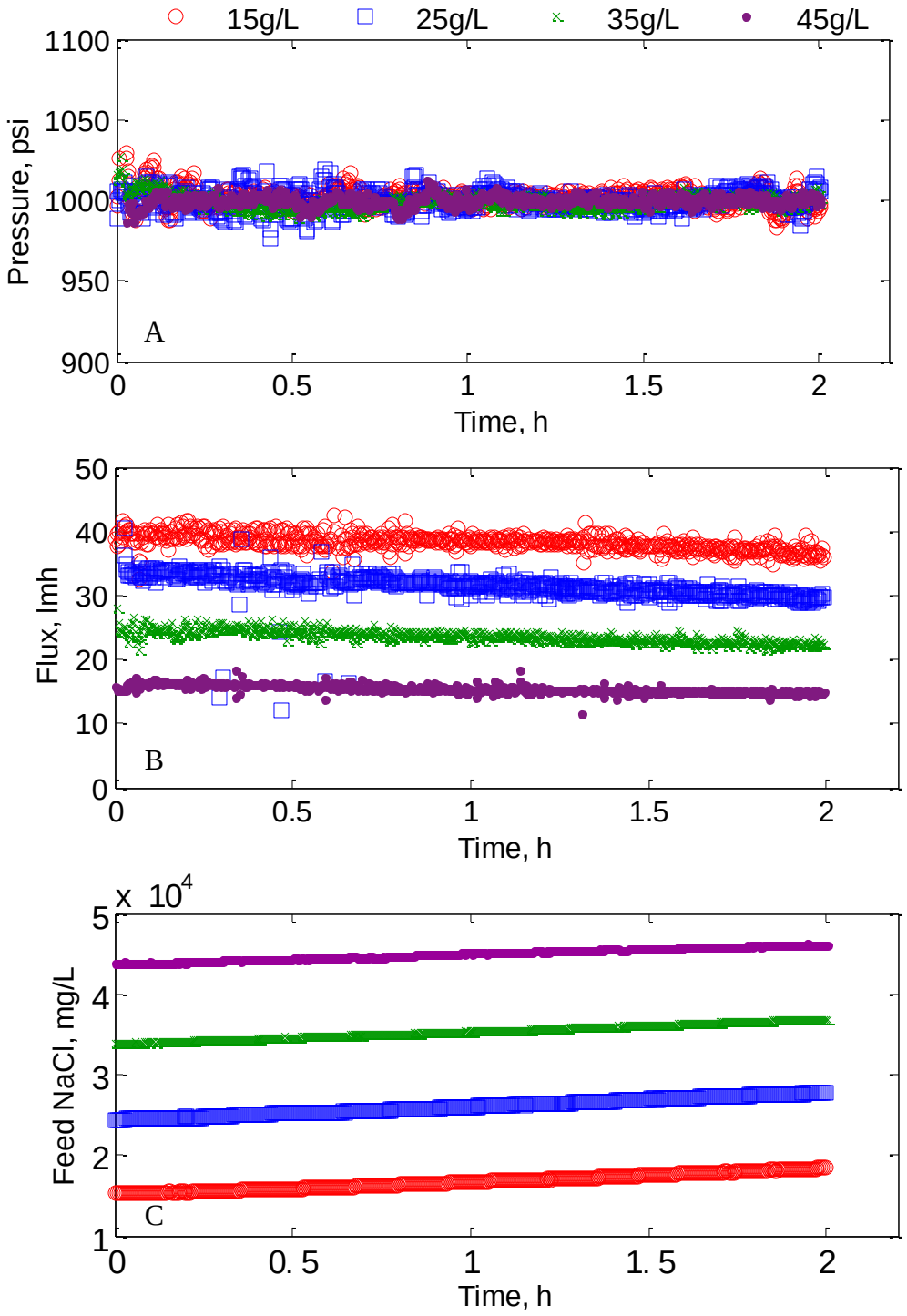
15g/L
25g/L
35g/L
45g/L
Pressure, psi
1100
1050
1000
950
900
A
0
0.5
1
1.5
2
Time, h
Flux, lmh
50
40
30
20
10
0
B
Time, h
x 10^4
Feed NaCl, mg/L
5
4
3
2
1
C
0
0. 5
1
1. 5
2
Time, h

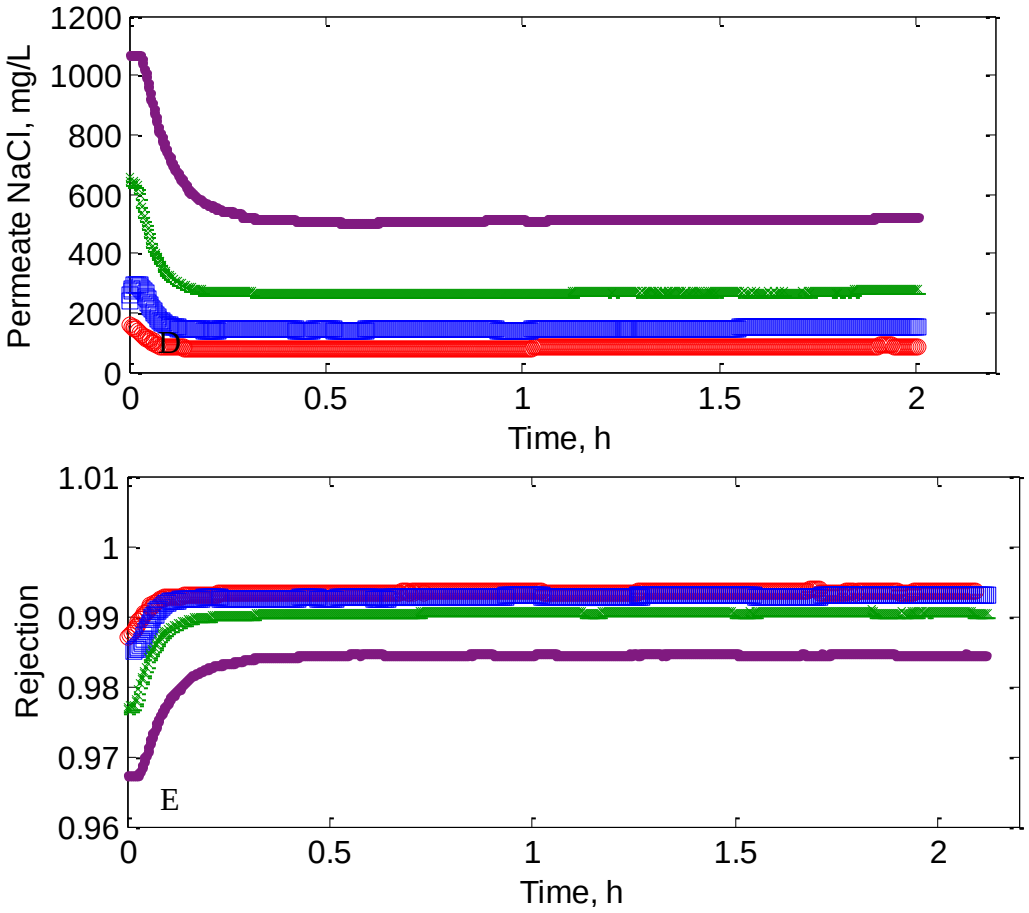

Figure 4.2.1 Wind-RO steady-state performance using feed water of 15, 25, 35, and 45 g/L NaCl plotted as (A) applied pressure; (B) flux; (C) feed NaCl; (D) permeate NaCl; (E) rejection.

4.2.2. Steady State Operation Characteristics Using Different Crossflow Velocities

In this section, steady-state operation characteristics were analyzed using three different crossflow velocities, 32 cm/sec, 47 cm/sec, and 61 cm/sec under 1000 psi steady state (Figure 4.2.2 (A)) with PV connected. The feed solution concentration used was 35 g/L and the initial air pressure was 400 psi.

The fluxes were around 25 lmh with all three different crossflow velocities, which was shown in Figure 4.2.2 (B). This could be explained by Equation [8]. In this set of

experiments, the feed solution, the membrane coupons and applied pressure were the same and there was no fouling, which means all the variables in the equation that could change flux value were kept constant. Therefore, the fluxes were about the same while only crossflow velocities were varied. There should have been a difference in concentration polarization due to the varying crossflow velocity, which should have changed the salt concentration at the membrane wall and thus changed the effective osmotic pressure felt by the membrane. But for the operating conditions used here there was little evidence from the flux numbers that the concentration polarization was different with different crossflow velocity.

$$N_{Aw} = (\Delta P - \Delta \pi)/[(Rm+Rc)\,\mu] \qquad [8]$$

In Equation 8, N_{Aw} is water flux, ΔP is transmembrane pressure, $\Delta \pi$ is the transmembrane osmotic pressure, Rm is resistance of the membrane (related to overall porosity), Rc is resistance of the cake (related to membrane fouling) and μ is liquid viscosity.

From Figure 4.2.2(C), rejection slightly increased as crossflow velocity increased, which is most noticable at the beginning of the runs. The reason might be because more shear force induced by higher crossflow velocity did have some small effect on concentration polarization.

In this study, high crossflow velocity did not show much benefit on improving the RO performance because the desalination process was only operated for 2 hours and no foulant was added in the feed solution. In real-world operation, high crossflow velocity

may decrease fouling problems. More experiments would be needed in the future to demonstrate this point.

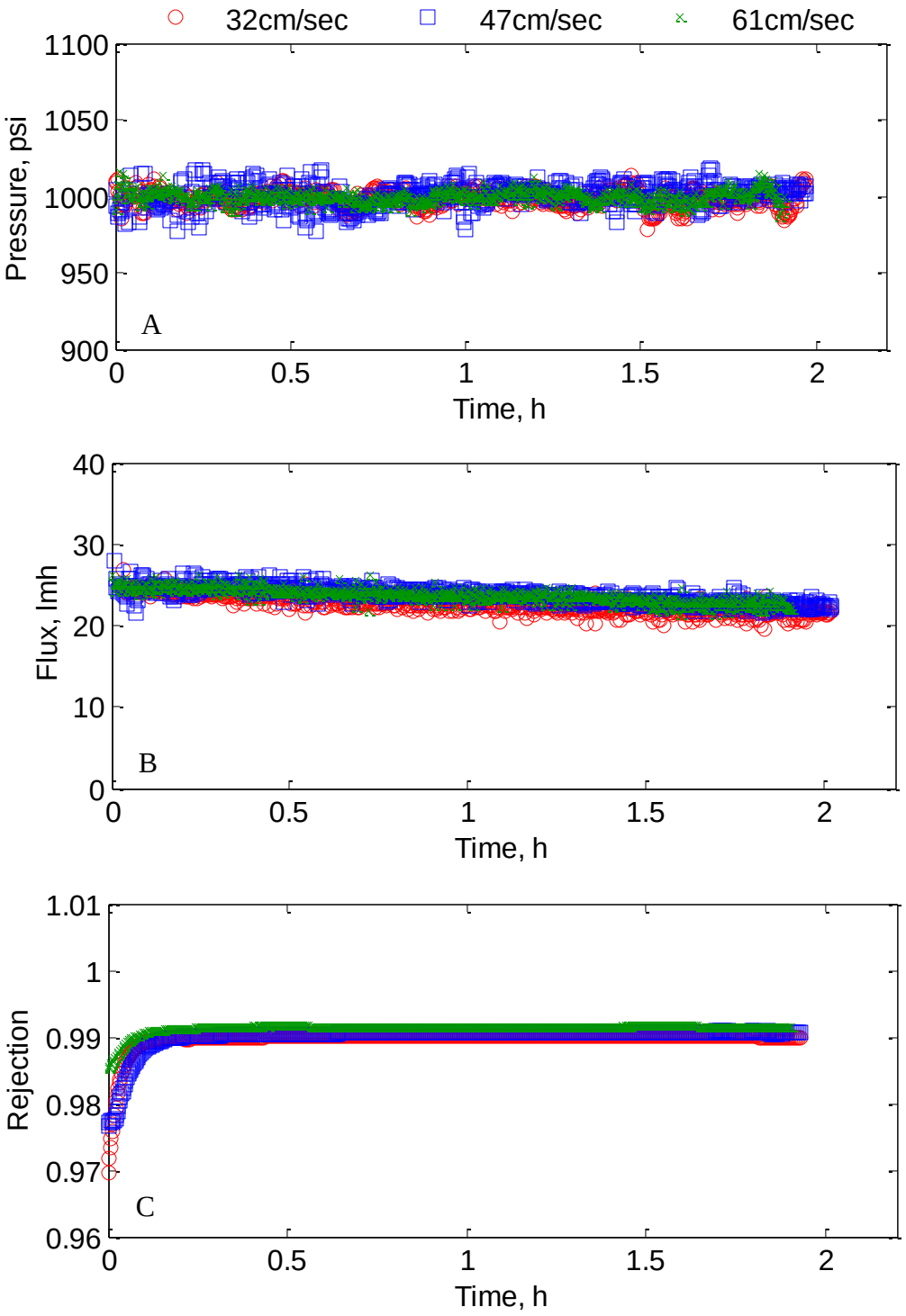

Figure 4.2.2 Wind-RO steady-state performance using 32, 47 and 61 cm/sec crossflow velocities plotted as (A) applied pressure; (B) fluxes; (C) rejection.

4.2.3. Steady-State Operation Characteristics Using Different Air:Water Ratios

The influence of different air:water ratios in the PV were analyzed by changing the pre-charged nitrogen pressure in the PV. The initial charged gas pressures used were 0, 200, 400, and 600 psi. The experiments were maintained at 1000 psi steady state for two hours. 47 cm/sec crossflow velocity and 35 g/L NaCl solutions were used as feed in these experiments.

From figure 4.2.3 A, steady-state pressure was well maintained at 1000 psi in all four experiments. In figure 4.2.3 B, the results showed the flux increased as initial charged gas pressure increased. The improvement of flux could be because of the dissolved nitrogen in the salt solution in the experiments. The osmotic pressure for nitrogen was zero since no ion was produced during the dissolving process, so nitrogen can go through the membrane very fast. The nitrogen passing through the membrane pores together with the water it dissolved in somehow caused an improvement in flux.

A significant improvement of flux was shown from initial air pressure of 200 psi to 400 psi. The reason was that a much larger amount of nitrogen was dissolved in salt solution under 400 psi initial gas pressure compared with the experiment under 200 psi initial air pressure. Nitrogen almost reached saturation in the salt solution with 400 psi initial gas pressure which was demonstrated in section 4.1.1, therefore, a small amount of nitrogen further dissolved in the salt solution under 600 psi initial air pressure. Very similar flux was achieved by 400 psi and 600 psi initial gas pressure. From figure 4.1.2 C, rejection was improved with the presence of pre-charged nitrogen. The rejection

increased with increased initial gas pressure of from 0 to 600 psi, while the rejection increased significantly when initial pressure increased from 200 psi to 400 psi.

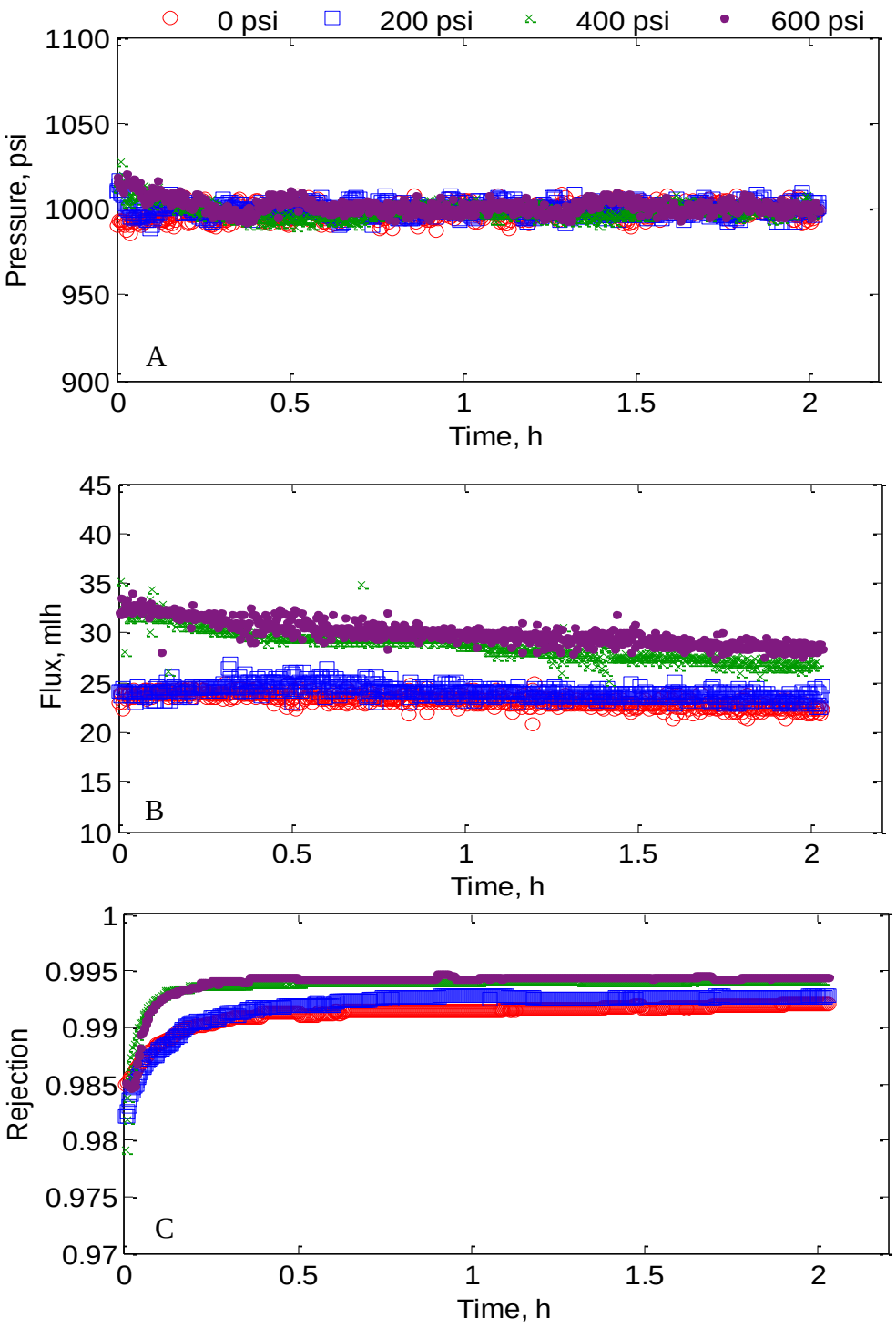

Figure 4.2.3 Steady-state performance under 0, 200, 400, and 600 psi initial air pressure. Pressure, fluxes and rejection are shown in figure A, B and C respectively.

4.3.Operational Characteristics under Batch Mode

Batch mode experiments were conducted to mimic the circumstance that wind power was not enough to drive desalination under steady state mode and permeate was produced without pumping in feed. Batch mode started at 1000 psi after a two hour steady-state run and was tested both without and with crossflow.

4.3.1. Batch Mode Operation Characteristics without Crossflow

Batch mode experiments without cossflow were conducted by isolating the PV after the 2 hour steady state run. Remaining pressure in the PV drove the desalination process. All experiments used 35 g/l NaCl feed solution and 400 psi initial air pressure. The experiments lasted 4 hours.

As it is shown in figure 4.3.1, fluxes and rejection deteriorated dramatically, even though the applied pressure remained high (above 950 psi). The salt concentration in the membrane test cell increased dramatically over time since no crossflow existed to remove salt from the cell. Also, under this “dead-end” mode, concentration polarization would have been high as no convective forces, but only diffusive forces, pulled salt away from the membrane. Less water and more salt molecules went through the membrane, which resulted in non-acceptable rejection results. According to EPA the secondary maximum contamination level for total dissolved solids is 500 mg/L. This means rejection should be at least 98.6% for the 35 g/L feed solution. However, the rejection in this experiment was below 98.6% except for during the short period in the beginning, which violated the regulation set by EPA. Therefore, this experiment demonstrated that crossflow is necessary to produce high quality drinking water by RO desalination. Also, if the wind

dies completely and no power is available to provide crossflow, the PV should be isolated without generating permeate to hold the energy for next start up.

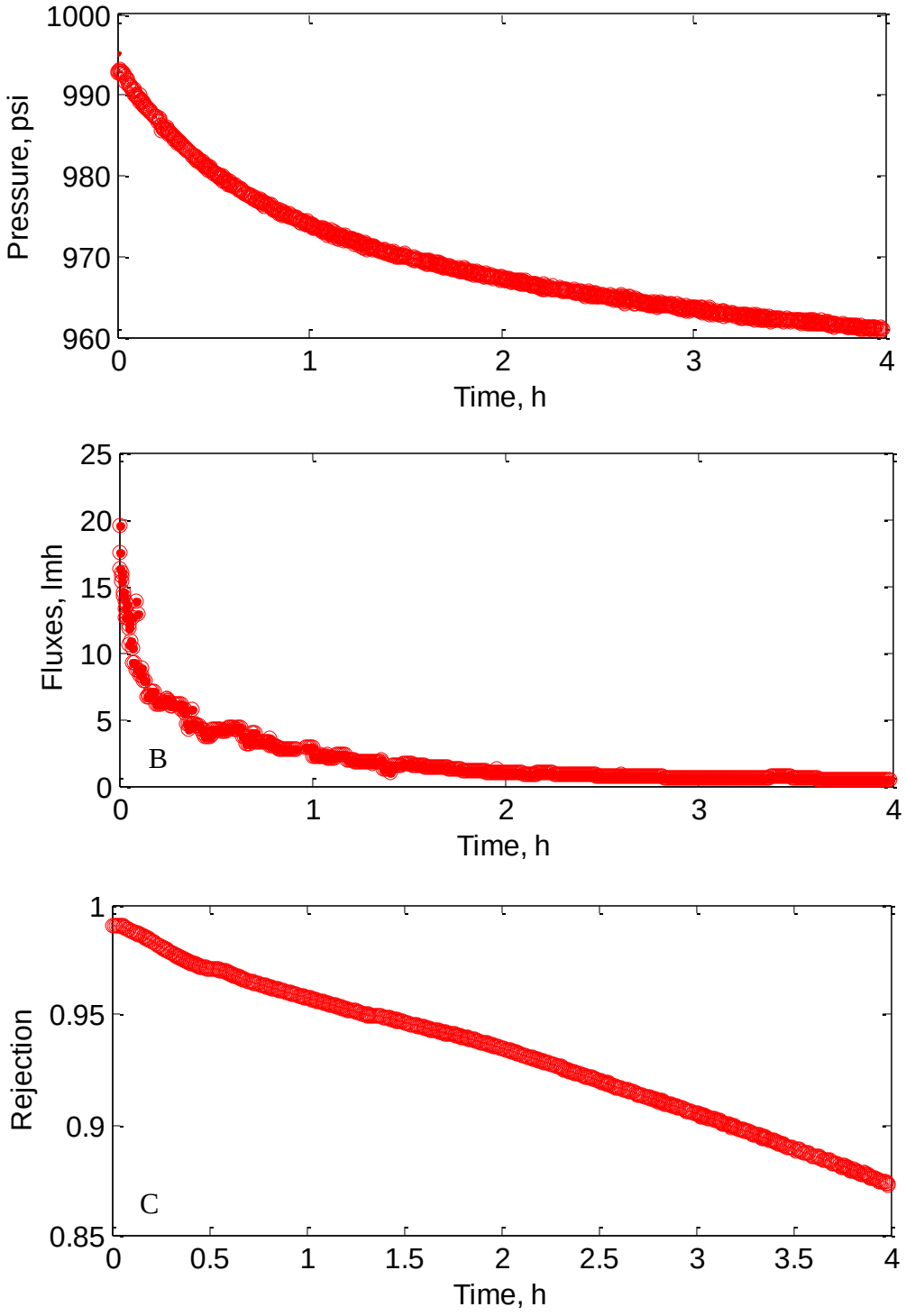

Figure 4.3.1 Wind-RO batch mode performance without crossflow plotted as (A) applied pressure; (B) flux; (C) rejection.

4.3.2. Batch Mode Operation Characteristics with Crossflow

Crossflow was generated by the pump outside the PV during batch mode experiments in this section. Performance under different feed concentration, crossflow velocities and air-water ratios were tested and the results were presented in the following sections.

4.3.2.1. Different Feed Concentrations

Three different feed concentrations, 15 g/l, 25 g/l and 35 g/L, were run under bench mode wind RO. The experiments were conducted using 47 cm/sec crossflow velocity and 400 psi initial air pressure.

The fluxes in this set of experiments were affected by feed concentration. As it is shown in Fig. 4.3.2.B, high feed concentration led to low flux due to the fact that from Equation 8, flux is inversely proportional to osmosis pressure difference ($\Delta\pi$) and $\Delta\pi$ is proportional to feed concentration. As permeate was produced, the pressure held in the PV was released, which resulted in decreasing applied pressure over time shown in Figure 4.3.2.B. Applied pressure decreased fastest with 15 g/L feed concentration because the most permeate was produced in this case. Decreasing applied pressure caused deteriorating flux over time in return. Pressure held in the PV was released slowest with the highest feed concentration (35 g/L) because less permeate was generated in the 35g/L experiment.

In Fig 4.3.2.C, highest rejection was achieved in the 15 g/L experiment, while the 35g/L experiment had the lowest rejection rate. The rejection for all three feed concentrations decreased over time. The explanation is shown in Equation 9; salt flux is

proportional to the difference between feed concentration and permeate concentration and compared to C_f , C_p is negligible, so salt flux is roughly proportional to C_f. C_f was increased in this experiment due to the fact that permeate was released and the concentrate was recycled back to the system. Therefore, high salt flux and low rejection is expected when high feed concentration is applied, and also the rejection is expected to decrease over time.

$$N_s = B (C_f - C_p) \quad [9]$$

In Equation 9, N_s is the salt flux through the membrane, B is the salt permeability constant describing the physical characteristics of the membrane, C_f is the salt concentration in the feed solution, and C_p is the salt concentration in the permeate solution.

As mentioned previously, the EPA-established secondary maximum contamination level for total dissolved solids is 500 mg/L, which means rejection should be at least 98.6%, 98.0% and 96.7% for 35 g/L, 25 g/L and 15 g/L feed solutions, respectively. From Figure 4.3.2.C, over 98.6% rejection was achieved by all three feed solution experiments, which means batch mode with crossflow can give rejections that comply with drinking water regulations.

Crossflow during batch mode can largely improve performance of the RO desalination process from the aspects of fluxes and rejection, compared with batch mode without crossflow presented in the last section. The energy needed to provide crossflow is very low compare to the energy used for providing applied pressure; hence, with the energy stored in the PV, the wind energy required to produce high quality drinking water

is significantly reduced, which makes the system still operational when low wind events occur.

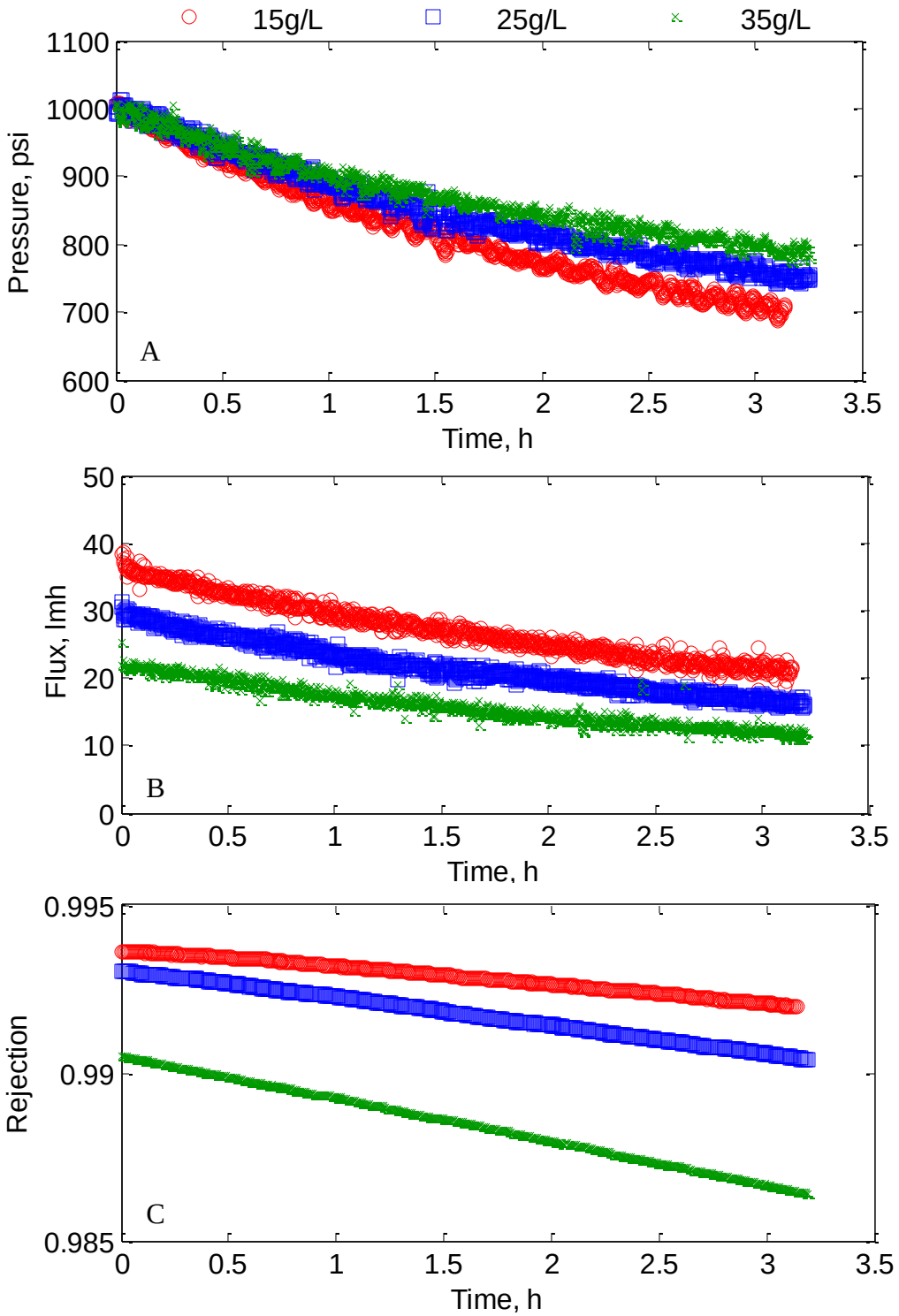

Figure 4.3.2 Wind-RO batch mode performance with different feed concentration plotted as (A) applied pressure; (B) fluxes; (C) rejection.

4.3.2.2. Different Crossflow Velocities

Three different crossflow velocities (32 cm/sec, 47 cm/sec, 61 cm/sec) were applied to check energy reduction possibilities in providing lower crossflow under batch mode. 35 g/L feed solution concentration and 400 psi initial air pressure were applied in this set of experiments.

From Fig 4.3.3, pressure and flux for all three experiments with different crossflow velocities followed the same pattern. The figure showed a slightly difference of rejection, but the difference was not significant and was within the range of 1%. Thus, crossflow velocity did not significantly affect the performance of the batch mode wind RO desalination process.

From these data, it is presumed that crossflow velocity can be lowered to further reduce the energy consumption during batch mode. In the real world operation, membrane fouling should be taken into consideration. In this case, a minimum crossflow velocity should be set to provide enough shear force to avoid fouling. More effort in this scenario should be made in the future to take into consider membrane fouling.

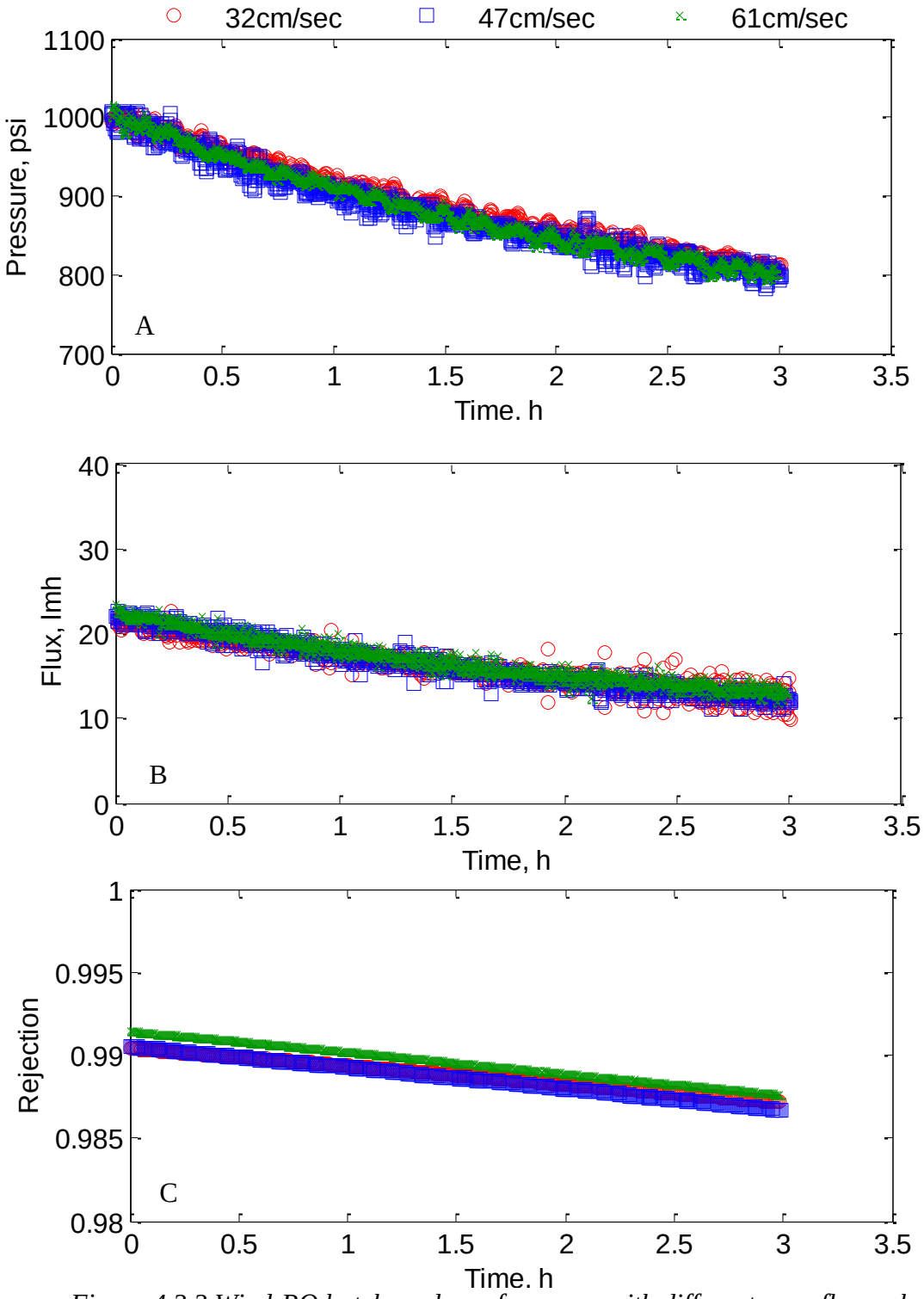

Figure 4.3.3 Wind-RO batch mode performance with different crossflow velocities plotted as (A) applied pressure; (B) fluxes; (C) rejection.

4.3.2.3. Different Air:Water Ratios

Different air:water ratios in the PV were tested by changing the pre-charged nitrogen pressure in the PV. Batch mode with crossflow was tested with different initial air pressure of 0, 200, 400, and 600 psi. Feed concentration and crossflow velocity were 35 g/L and 47 cm/sec respectively.

From Fig 4.3.4.A, as permeate was released, pressure held in the PV decreased overtime, but with different initial air pressure, the pressure followed different patterns. Slowest pressure dropping was observed with highest initial air pressure (600 psi). This phenomenon demonstrated that air pressurized PV can provide energy buffer for desalination process and also the higher the air:water ratio, the more capacity the energy buffer has.

From Fig 4.3.4 B, higher flux was generated with the presence of larger air content in the PV. Besides, less energy was consumed per unit permeate produced when higher initial air pressure was applied because pressure dropped slower in this case. From 4.3.4 C, rejection deterioration was slowed down with high initial air pressure. The reason is that higher pressure in the PV was maintained with higher initial air pressure and higher feed pressure pushed water through the membrane at a faster rate than salt can be transported.

Under batch mode, higher initial air pressure can provide more energy buffer capacity, which leads to largely improved water quantity and quality.

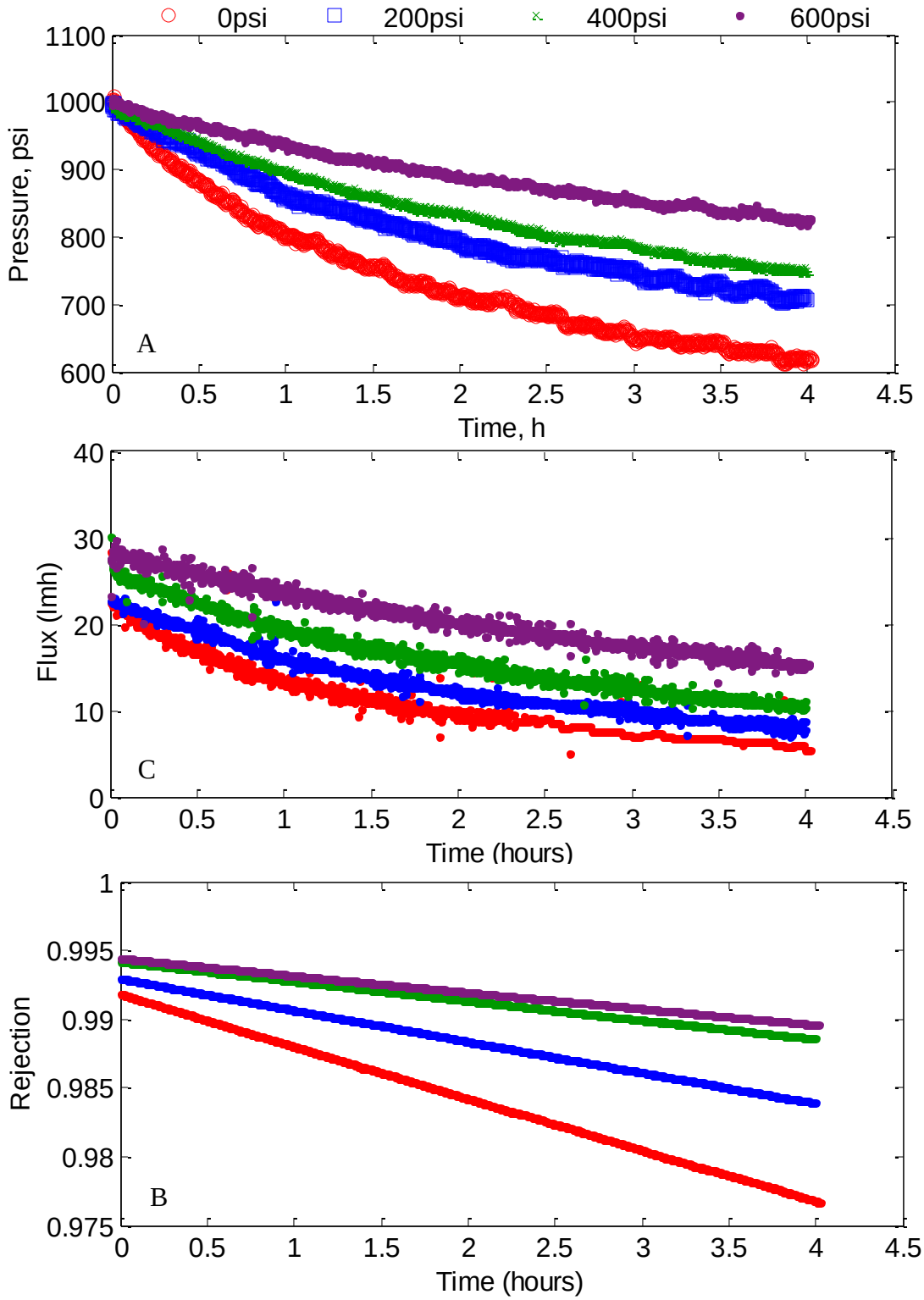

Figure 4.3.4 Wind-RO batch mode performance with different air-water ratios plotted as (A) applied pressure; (B) flux; (C) rejection.

4.4. Effects of Simulated Fluctuations

Three sets of experiments were conducted to test the performance of Wind-RO with PV under fluctuation conditions. Wind fluctuation was mimicked by varying the pump speed which was enabled by reprogramming the pump speed control in LabVIEW. The average pump speed was 6.4Hz and the peak to peak amplitude was 1.6 Hz. All the experiments started with 1000 psi steady state for 30 mins followed by two hours run under simulated fluctuation mode. Salt solutions with 35 g/L concentration and 400 psi initial air pressure were used.

4.4.1. Fluctuating Operations without Actuator Control

The actuator was disabled during the fluctuating period and the concentrate valve position remained the same as during the steady state period. Without actuator trying to keep up the target pressure, a baseline was set for fluctuating operation. The period of cosine wave was set at 5 mins. The experiment bypassing the PV (conventional RO) was run as control, while initial air pressures were varied.

Fig 4.4.1.A shows the variation of applied pressure was largely reduced with the energy buffer provided by the PV. High air:water ratio delivered high buffer capacity, which led to a much more stable desalination performance. Without actuator pressure control, the average pressure of all 5 experiments all dropped from 950 psi to 700 psi and stabilized. There was a significant stabilization improvement from 0 initial air pressure to 200 initial air pressure, but the performance was only further improved a little with increasing initial air pressure. Also, as it is shown in Fig. 4.1.1.B, flux varied in the same

manner as applied pressure with different air:water ratios. From the aspect of applied pressure and fluxes, 200 psi initial air pressure can provide enough energy buffer to minimize applied pressure variation, which led to a largely reduced variability in flux.

Fig. 4.1.1 C shows rejection change under fluctuating power supply. It was observed that experiments with 400 psi and 600 psi initial air pressure had higher rejections than conventional RO rejection, while experiments with 0 psi and 200 psi initial air pressure had lower rejections than conventional RO. Dampened applied pressure fluctuation by the energy buffer provided by the PV should improve membrane rejection performance. Hence, conventional RO was supposed to deliver the worst rejection, but the rejection of the conventional RO experiment was higher than the 200 psi initial air pressure experiment. The reason for this result remains unknown. Except for conventional RO, the rejection followed the trend that high initial air pressure led to high rejection.

Overall, 600 psi initial air pressure delivered the best RO desalination performance including largely dampening variation of applied pressure and giving the highest flux and rejection. On the other hand, the experiments showed the potential of lowering the applied pressure to as low as 700 psi to deliver high quality drinking water.

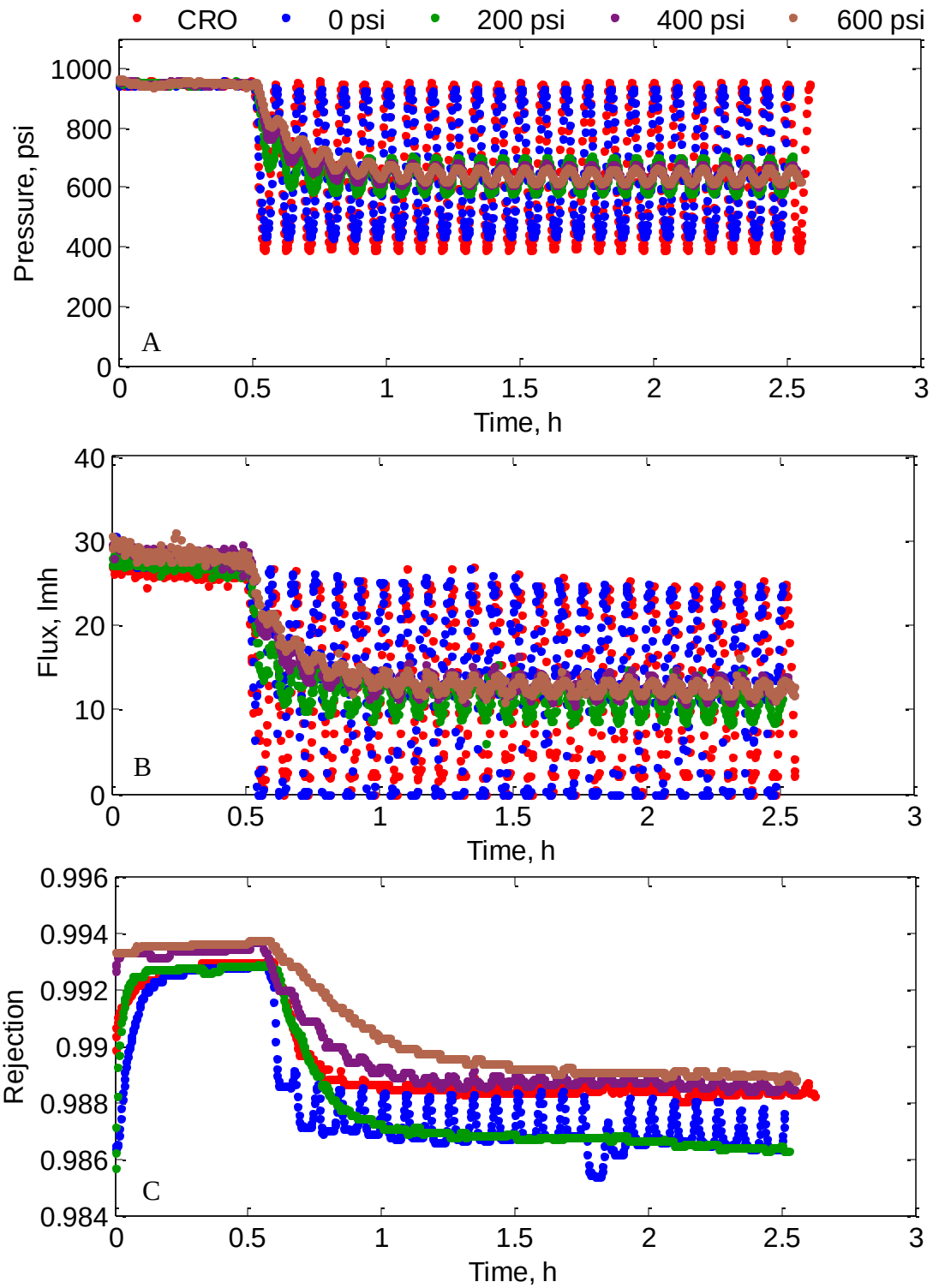

Figure 4.4.1 Fluctuating operations under both conventional RO and wind RO conditions with constant actuator voltage plotted as (A) applied pressure; (B) flux; (C) rejection. (CRO: conventional RO, with the PV bypassed)

4.4.2. Fluctuating Operations with Target Pressure of 950 psi

In this section, the actuator pressure control was enabled during the fluctuating period to keep a target pressure of 950 psi. The actuator control in LabVIEW was reprogrammed in order to let the actuator react quickly enough to maintain the target pressure.

From 4.4.2. A, compared with conventional RO operation, the energy buffer provided by the PV in this case induced even higher pressure fluctuation. The reason lay in the fact that with high energy buffer capacity in 400 psi and 600 psi experiments, the system reacted much more slowly to the actuator. Once pressure increased beyond the set point, the actuator opened the concentrate valve, but the pressure was not released quickly; the energy buffer maintained the pressure at a high level. The pump, however, changed immediately and caused an over-pressure situation. Similarly for the low-pressure case, the system did not build up pressure as quickly as the pump decreased its flow, so a low-pressure situation occurred. These high and low-pressure oscillations continued throughout the experiments. Conversely, with the low applied air pressure and conventional RO cases, the system pressurized and depressurized quickly in response to the actuator's needle valve control because the energy buffer was low or none

As it is shown in Fig. 4.1.2.B, flux differences were not significant, but flux fluctuation still increased as the air:water ratio increased. Fluxes of conventional RO varied in about the same manner as fluxes with 200 psi initial air pressure, but these varied much less than fluxes with 400 psi and 600 psi initial air pressure. The reason is the same as was explained in last paragraph for applied pressure.

From Fig. 4.1.2.C, rejection with 400 psi and 600 psi initial air pressure was lower than rejection of conventional RO, while rejection with 200 psi initial air pressure was slightly higher than rejection of conventional RO. However, the rejections were all above 98.6% and met EPA drinking water requirements.

The actuator control showed opposite effects on the experiments with high energy buffer capacities (400 and 600 psi initial air pressure) and only slightly improved the performance of the experiment with low energy buffer capacity (200 psi initial air pressure). Hence, with energy buffer provided by PV, actuator pressure control is not capable of delivering good performance under fluctuating conditions.

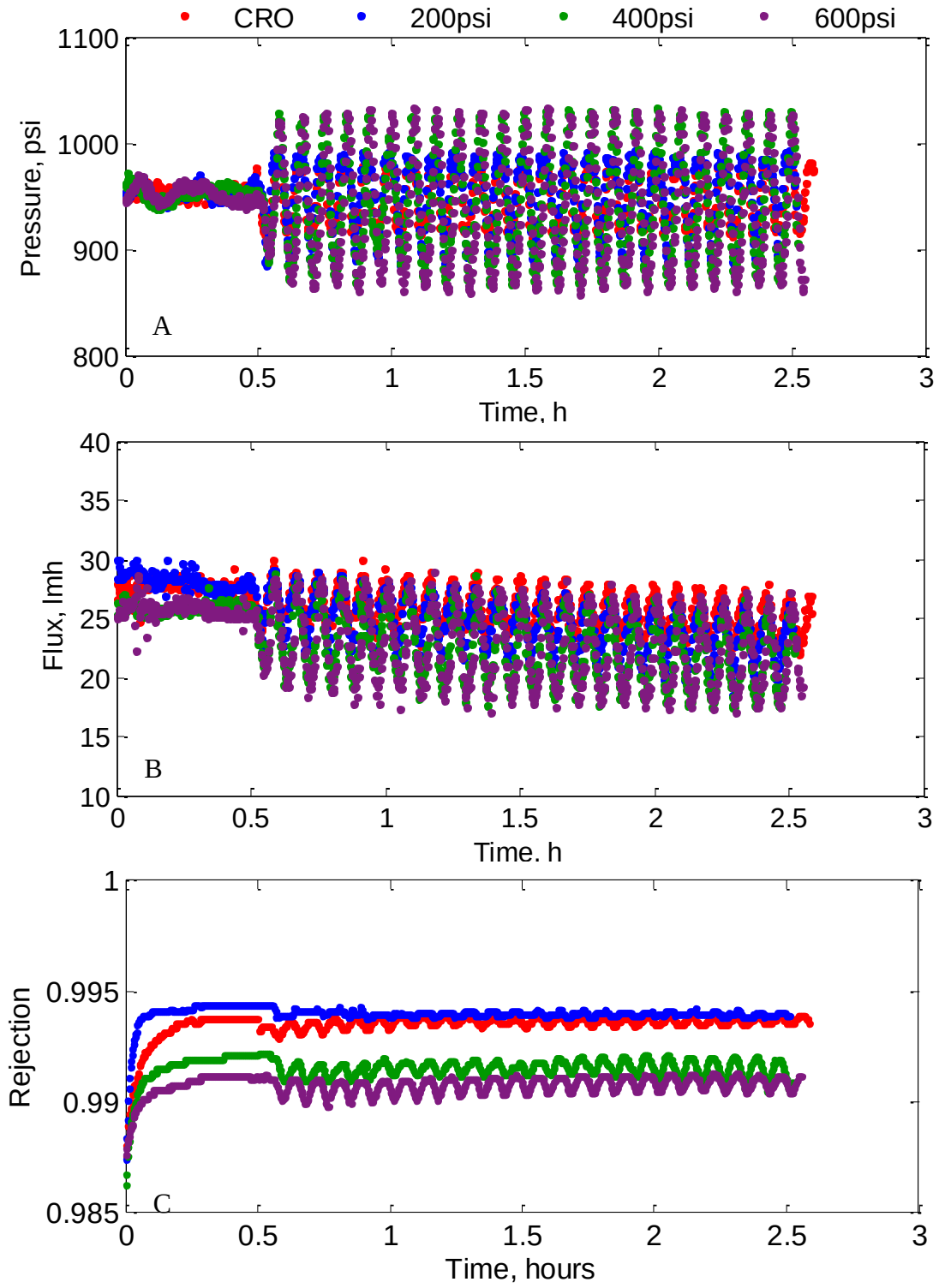

Figure 4.4.2 Fluctuating operations under both conventional RO and wind RO conditions with 950 psi target pressure plotted as (A) applied pressure; (B) flux; (C) rejection.

4.4.3. Fluctuating Operations with Different Periods

In this set of experiments, the period of oscillation was varied, in order to observe the performances under different wind patterns. Four different oscillation periods were 2.5, 5, 7.5 and 10 mins. Initial air pressure of 400 psi was used in this set of experiments. The actuator was also enabled with the target pressure at 950 psi.

From Fig. 4.4.3, the variation range of pressure, flux and rejection were the same under simulated wind pattern with 2.5, 7.5 and 10 min periods, but pressure, flux and rejection fluctuated stronger under the 5-min period wind pattern. The reason lies in the difference in way the system was operated, but not the different periods. The experiment using 5 mins period was conducted in section 4.4.2, which used 50 psi increment for actuator pressure control, while the other three experiments were conducted using 30 psi increment. The rejections of all four experiments were higher than 98.6%, which complied with EPA drinking water secondary regulation.

Thus, the performance of wind RO desalination coupled with the energy storage device stayed the same no matter the period change of wind variation. Besides, by reducing the pressure increment, there is potential of further reducing the negative effects of fluctuation wind power on the performance of wind RO desalination.

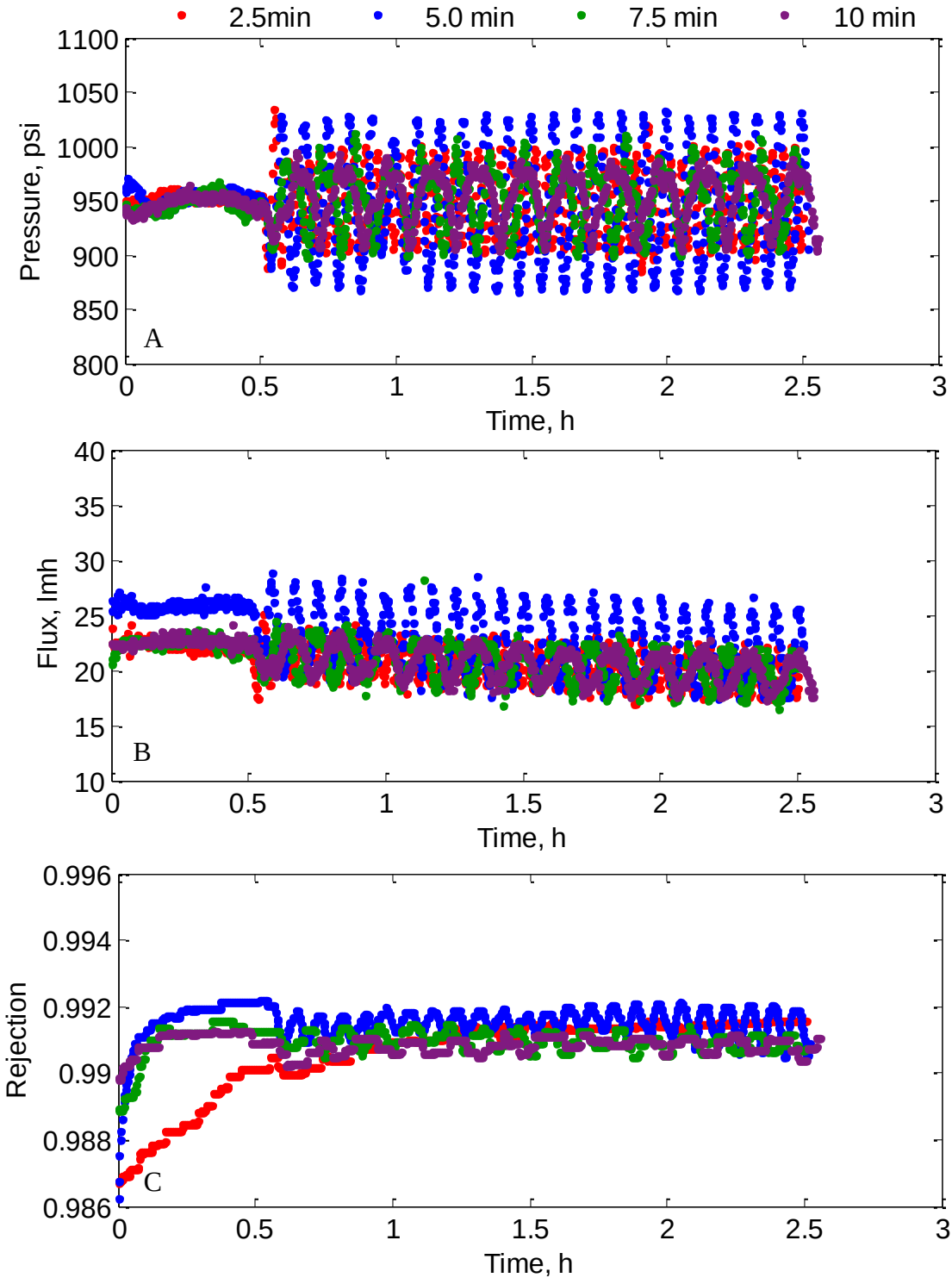

Figure 4.4.3 Fluctuating operations following 2.5, 5, 7.5, and 10 mins period sinusoidal profile plotted as (A) applied pressure; (B) fluxes; (C) rejection.

4.5. Effects of Intermittent Operation

Simulated wind intermittence was used to further test the performance of this system with air pressure as an energy storage buffer. Intermittent operation was simulated by turning the pump off for 5 mins and restarting the system afterwards. Sufficient time was given for the system parameters to return to their original values after the period of no power. The experiments were conducted under four scenarios: conventional RO without power for crossflow during the wind off time, conventional RO with power for crossflow during the wind off time, wind RO without power for crossflow during the wind off time, and wind RO with power for crossflow during the wind off time. The detailed explanation of these four scenarios is in section 3.5.5.

Fig. 4.5.1.A shows that the pressure was totally released in conventional RO experiments no matter with or without crossflow, while pressure in the experiments with the PV remained near 1000 psi. The energy was stored in the PV when the wind power died, which saves the energy of re-pressurizing the desalination system and allows the system to desalinate even though wind power is not available.

No permeate was produced under conventional RO operation when power input stopped because the pressure was released totally. The rejection of the conventional RO experiment started at a much lower value than rejection of wind RO did when power started up.

Without power to provide crossflow, flux and rejection in wind RO experiment deteriorated significantly, while flux and rejection remained about the same with crossflow. This effect was caused by the fact that the crossflow can continue removing

salts from the membrane cell, while with no crossflow the salts are not removed and the concentration increases greatly.

Overall, wind RO desalination with the energy storage device showed a significant advantage over conventional RO under intermittent wind operation in the following two aspects: 1) the PV can store whatever energy was in it before the wind stopped without wasting it and 2) the energy stored in the PV can drive RO desalination process to produce good quality drinking water when a small amount of wind energy (or perhaps a low-power grid electricity source) is available to provide crossflow.

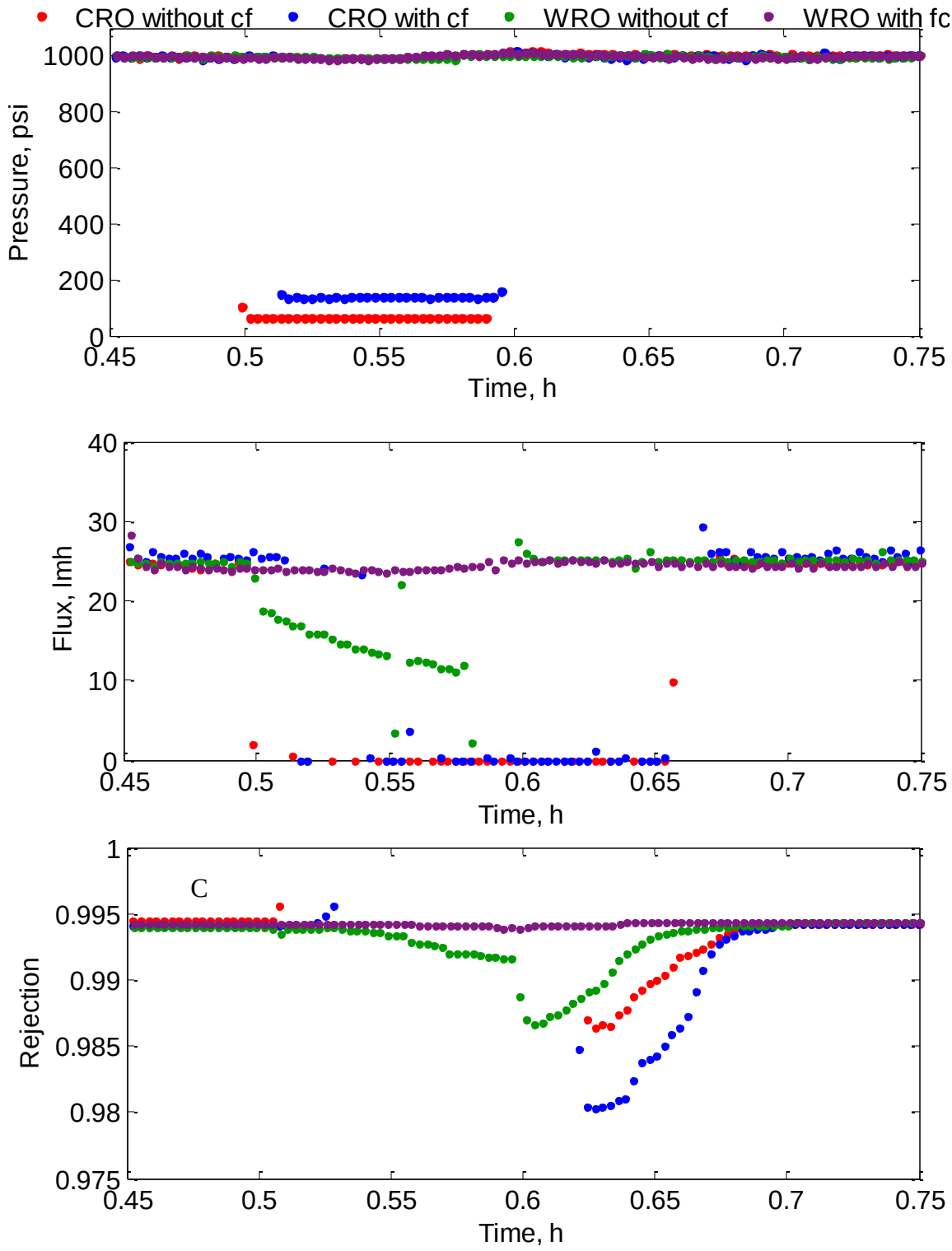

Figure 4.5.1 Four different intermittent wind operations plotted as (A) applied pressure; (B) flux; (C) rejection

CHAPTER 5 CONCLUSIONS AND FUTURE WORK

The aim of this thesis project was to conduct a feasibility bench-scale study of an RO desalination system that could be driven by wind energy. The challenge lies in using fluctuating and intermittent wind energy to drive the RO desalination process which usually requires constant power input. To enable efficient RO operation using variable wind energy, a PV containing compressed air serves as an energy storage device which drives RO desalination process when wind energy dies down. It also serves to dampen the wind energy fluctuations.

The effects of dissolved nitrogen under high pressure on the RO process were evaluated by conducting bench scale experiments. It was estimated that 0.86 g/L nitrogen was dissolved in the salt solution after the four-hour 1000 psi steady-state experiment when 400 psi initial gas pressure was applied. Compared to the theoretical nitrogen dissolution of 1.19 g/L, it did not reach the nitrogen saturation point under this experimental condition. Higher initial air pressure will result in a higher amount of gas dissolved in the feed solution. The rejection and fluxes of steady-state experiments under both CRO and WRO using 400 psi initial air pressure were compared and indicated that the dissolved nitrogen impacts on fluxes did not show a clear trend, but caused a slight improvement on rejection under feed concentration from 0 to 45 g/L.

The WRO steady state experiments were conducted to set a baseline for the batch mode and simulated fluctuating/intermittent WRO experiments. Good fluxes and high rejection (>98.6%) were achieved for all three feed concentrations (15, 25, and 35 g/L) using 400 psi initial air pressure, which demonstrated that WRO coupling with PV is

suitable to treat both brackish water and seawater. Crossflow velocity was varied from 32 cm/sec to 61 cm/sec, but no improvement of rejection or flux was shown with high crossflow velocity. Therefore, low crossflow velocity can be applied to further lower the energy consumption as long as no desalination performance deterioration is observed. In the real world operation, membrane fouling should be taken into consideration. In this case, a minimum crossflow velocity should be set to provide enough shear force to avoid fouling. More effort in this scenario should be made in the future to take fouling into consideration. Different initial air pressures, 0, 200, 400 and 600 psi, were applied when 35 g/L feed solution was used and the results showed that 600 psi initial air pressure delivered the highest fluxes and rejection. Hence, increasing initial air pressure can help to improve the performance of WRO desalination.

Batch mode experiments were conducted to mimic the circumstance that wind power was not enough to drive desalination under steady state mode and permeate was produced without pumping in feed. Both the flux and rejection deteriorated too much without crossflow under batch mode operation. The conclusion was that crossflow was necessary to produce high quality drinking water by RO desalination. When wind stops completely and no other power sources are available to provide crossflow, the PV should be isolated without generating permeate to hold the energy until wind picks up. On the other hand, crossflow largely improved performance of RO desalination process from the aspects of fluxes and rejection, compared with batch mode without crossflow. But, the magnitude of crossflow velocity did affect the performance of bench mode WRO, thus, crossflow velocity can be lowered to save energy. Initial air pressure was varied and the

conclusion was that the highest initial air pressure (600 psi) can provide the highest energy buffer capacity, which leads to largely improved fluxes, water quality and saving energy at the same time.

Bench-scale experiments were also conducted under simulated fluctuation conditions. In the experiments without pressure control, the highest initial air pressure (600 psi) delivered the best WRO performance including largely dampening variation of applied pressure and giving the highest flux and rejection. The experiments also showed high quality drinking water can be produced under applied pressure as low as 700 psi, so the applied pressure can be lowered to reduce energy consumption. The experiments with pressure control which try to keep up the target pressure of 950 psi were conducted. Comparing with CRO, the performance was improved slightly with 200 psi initial air pressure, but worsened under 400 and 600 psi initial air pressure from the aspect of dampening the fluctuation, and fluxes and rejection improvement. Therefore, with an energy buffer provided by the PV, actuator pressure control is not necessary to deliver good performance under fluctuating conditions. The period of cosine oscillation was varied in order to observe the performance under different wind patterns. The conclusion is that the fluxes and rejection stayed about the same with different periods and by reducing the pressure increment, the fluctuation of applied pressure can be further minimized which can lead to better WRO performance.

Experiments were also conducted to test the performance of WRO under simulated intermittent wind conditions. WRO showed significant advantage over CRO in that PV can store the energy when the wind dies down and the stored energy can be used

to produce good quality drinking water when a small amount of energy is available to provide crossflow.

In the future, to simulate real wind power operation, real wind data should be obtained to run more real-world conditions. An example of a source of wind energy data is the Kansas State University Wind Turbine website (Kansas State University 2013). The length of the data can be tailored to two hours in order to compare to the experiments performed previously. High wind and low wind periods can be chosen. The power from the wind can be calculated and converted to pump speed. The performance of the bench-scale system under these conditions can provide another step in the proof of concept for the feasibility of this design using actual wind.

REFERENCES

Abdallah, S., Abu-Hilal, M., Mohsen, M. S. (2005). "Performance of a Photovoltaic Powered Reverse Osmosis System Under Local Climatic Conditions." *Desalination,* 183(1–3), 95-104.

Ackermann, T., and Söder, L. (2002). "An Overview of Wind Energy-Status 2002." *Renewable and Sustainable Energy Reviews,* 6(1–2), 67-127.

Androwski, J., Springer, A., Acker, T., Manone, M. (2011). "Wind-Powered Desalination: An Estimate of Saline Groundwater in the United States1." *JAWRA Journal of the American Water Resources Association,* 47(1), 93-102.

Ben Ali, I., Turki, M., Belhadj, J., Roboam, X. (2012). "Energy management of a reverse osmosis desalination process powered by renewable energy sources." *Proc., Electrotechnical Conference (MELECON), 2012 16th IEEE Mediterranean,* 800-805.

Carta, J. A., González, J., Subiela, V. (2003). "Operational Analysis of an Innovative Wind Powered Reverse Osmosis System Installed in the Canary Islands." *Solar Energy,* 75(2), 153-168.

Charcosset, C. (2009). "A Review of Membrane Processes and Renewable Energies for Desalination." *Desalination,* 245(1-3), 214-231.

Chen, J. (2011). "Development of Offshore Wind Power in China." *Renewable and Sustainable Energy Reviews,* 15(9), 5013-5020.

Colombo, D., de Gerloni, M., Reali, M. (1999). "An Energy-Efficient Submarine Desalination Plant." *Desalination,* 122(2–3), 171-176.

De Almaeida, A., and Moura, P. (2007). "Desalination with Wind and Wave Power." *Solar Desalination for the 21st Century,*18, 305-325.

Dehmas, D. A., Kherba, N., Hacene, F. B., Merzouk, N. K., Merzouk, M., Mahmoudi, H., Goosen, M. F. A. (2011). "On the Use of Wind Energy to Power Reverse Osmosis Desalination Plant: A Case Study from Ténès (Algeria)." *Renewable and Sustainable Energy Reviews,* 15(2), 956-963.

El-Ghonemy, A. M. K. (2012). "Water Desalination Systems Powered by Renewable Energy Sources: Review." *Renewable and Sustainable Energy Reviews,* 16(3), 1537-1556.

Eltawil, M. A., Zhengming, Z., Yuan, L. (2009). "A Review of Renewable Energy Technologies Integrated with Desalination Systems." *Renewable and Sustainable Energy Reviews,* 13(9), 2245-2262.

Folley, M., Peñate Suarez, B., Whittaker, T. (2008). "An Autonomous Wave-Powered Desalination System." *Desalination,* 220(1–3), 412-421.

Food and Agriculture Organization of the United Nations. (2000). "The FAOSTAT Database, Population: Annual Time Series." *Rome: Food and Agriculture Organization of the United Nations*.

Forstmeier, M., Mannerheim, F., D'Amato, F., Shah, M., Liu, Y., Baldea, M., Stella, A. (2007). "Feasibility Study on Wind-Powered Desalination." *Desalination,* 203(1-3), 463-470.

Fritzmann, C., Löwenberg, J., Wintgens, T., Melin, T. (2007). "State-of-the-Art of Reverse Osmosis Desalination." *Desalination,* 216(1-3), 1-76.

García-Rodríguez, L. (2003). "Renewable Energy Applications in Desalination: State of the Art." *Solar Energy,* 75(5), 381-393.

García-Rodríguez, L. (2002). "Seawater Desalination Driven by Renewable Energies: A Review." *Desalination,* 143(2), 103-113.

Gilau, A. M., and Small, M. J. (2008). "Designing Cost-Effective Seawater Reverse Osmosis System Under Optimal Energy Options." *Renewable Energy,* 33(4), 617-630.

Goosen, M., Mahmoudi, H., Ghaffour, N., Sablani, S. (2011). "Application of Renewable Energies for Water Desalination." *INTECH,* Open Access Publisher (Vienna, Austria), 30.

Greenlee, L. F., Lawler, D. F., Freeman, B. D., Marrot, B., Moulin, P. (2009). "Reverse Osmosis Desalination: Water Sources, Technology, and Today's Challenges." *Water Res.,* 43(9), 2317-2348.

Gude, V. G., Nirmalakhandan, N., Deng, S. (2010). "Renewable and Sustainable Approaches for Desalination." *Renewable and Sustainable Energy Reviews,* 14(9), 2641-2654.

Habali, S. M., and Saleh, I. A. (1994). "Design of Stand-Alone Brackish Water Desalination Wind Energy System for Jordan." *Solar Energy,* 52(6), 525-532.

Hanafi, A. (1994). "Desalination using Renewable Energy-Sources." *Desalination,* 97(1-3), 339-352.

Infield, D. (1997). "Performance Analysis of a Small Wind Powered Reverse Osmosis Plant." *Solar Energy*, 61(6), 415-421.

Joselin Herbert, G. M., Iniyan, S., Sreevalsan, E., Rajapandian, S. (2007). "A Review of Wind Energy Technologies." *Renewable and Sustainable Energy Reviews,* 11(6), 1117-1145.

Kaldellis, J. K., Kavadias, K. A., Kondili, E. (2004). "Renewable Energy Desalination Plants for the Greek islands—technical and Economic Considerations." *Desalination*, 170(2), 187-203.

Kalogirou, S. A. (2005). "Seawater Desalination using Renewable Energy Sources." *Progress in Energy and Combustion Science*, 31(3), 242-281.

Kamal, I., and Tusel, G. F. (1982). "An Evaluation of the Energy Requirements of Desalination Processes on the Basis of the Fuel-use Performance Ratio." *Desalination*, 40(3), 283-295.

Kansas State University. (2013). "Kansas state university wind turbine ." <http://wind-for-schools.caesenergy.org/windforschoolsweb/kansas_state.html> (03, 2013).

Karagiannis, I. C., and Soldatos, P. G. (2008). "Water Desalination Cost Literature: Review and Assessment." *Desalination,* 223(1–3), 448-456.

Kiranoudis, C. T., Voros, N. G., Maroulis, Z. B. (1997). "Wind Energy Exploitation for Reverse Osmosis Desalination Plants." *Desalination,* 109(2), 195-209.

Ladner, D. A., Subramani, A., Kumar, M., Adham, S. S., Clark, M. M. (2010). "Bench-Scale Evaluation of Seawater Desalination by Reverse Osmosis." *Desalination,* 250(2), 490-499.

Ladner, D. A. (2009). "Effects of Bloom-Forming Algae on Fouling of Integrated Membrane Systems in Seawater Desalination." *PhD Dissertation, University of Illinois at Urbana-Champaign*.

Lising, E., and Alward, R. (1972). "Unsteady State Operation of a Reverse-Osmosis Desalination Unit." *Desalination,* 11(3), 261-268.

Liu, C. C. K., Jae-Woo, P., Migita, R., Gang, Q. (2002). "Experiments of a Prototype Wind-Driven Reverse Osmosis Desalination System with Feedback Control." *Desalination*, 150(3), 277-287.

Ma, Q., and Lu, H. (2011). "Wind Energy Technologies Integrated with Desalination Systems: Review and State-of-the-Art." *Desalination,* 277(1–3), 274-280.

Mathioulakis, E., Belessiotis, V., Delyannis, E. (2007). "Desalination by using Alternative Energy: Review and State-of-the-Art." *Desalination,* 203(1-3), 346-365.

Miranda, M. S., and Infield, D. (2003). "A Wind-Powered Seawater Reverse-Osmosis System without Batteries." *Desalination,* 153(1–3), 9-16.

Mohamed, E. S., and Papadakis, G. (2004). "Design, Simulation and Economic Analysis of a Stand-Alone Reverse Osmosis Desalination Unit Powered by Wind Turbines and Photovoltaics." *Desalination,* 164(1), 87-97.

Park, G. L., Schäfer, A. I., Richards, B. S. (2009). "Potential of Wind-Powered Renewable Energy Membrane Systems for Ghana." *Desalination,* 248(1–3), 169-176.

Peñate, B., and García-Rodríguez, L. (2012). "Current Trends and Future Prospects in the Design of Seawater Reverse Osmosis Desalination Technology." *Desalination,* 284(0), 1-8.

Raluy, R. G., Serra, L., Uche, J. (2005). "Life Cycle Assessment of Desalination Technologies Integrated with Renewable Energies." *Desalination,* 183(1-3), 81-93.

Rosen, A., and Sheinman, Y. (1996). "The Power Fluctuations of a Wind Turbine." *J. Wind Eng. Ind. Aerodyn.,* 59(1), 51-68.

Subiela, V. J., de la Fuente, J. A., Piernavieja, G., Penate, B. (2009). "Canary Islands Institute of Technology (ITC) Experiences in Desalination with Renewable Energies (1996-2008)." *Desalin. Water Treat.,* 7(1-3), 220-235.

Subramani, A., Badruzzaman, M., Oppenheimer, J., Jacangelo, J. G. (2011). "Energy Minimization Strategies and Renewable Energy Utilization for Desalination: A Review." *Water Res.,* 45(5), 1907-1920.

Tarnacki, K., Meneses, M., Melin, T., van Medevoort, J., Jansen, A. (2012). "Environmental Assessment of Desalination Processes: Reverse Osmosis and Memstill®." *Desalination,* 296(0), 69-80.

Tzen, E. (2009). "Wind and Wave Energy for Reverse Osmosis." , 213-245.

Tzen, E., and Morris, R. (2003). "Renewable Energy Sources for Desalination." *Solar Energy*, 75(5), 375-379.

Veza, J. M. (2001). "Desalination in the Canary Islands: An Update." *Desalination*, 133(3), 259-270.

Voivontas, D., Misirlis, K., Manoli, E., Arampatzis, G., Assimacopoulos, D. (2001). "A Tool for the Design of Desalination Plants Powered by Renewable Energies." *Desalination*, 133(2), 175-198.

Warfel, C. G., Manwell, J. F., McGowan, J. G. (1988). "Techno-Economic Study of Autonomous Wind Driven Reverse Osmosis Desalination Systems." *Solar & Wind Technology*, 5(5), 549-561.

World Health Organization. (1973). "International Standards for Drinking Water." *Geneva*, 3rd ed. Ed., .

Zejli, D., Benchrifa, R., Bennouna, A., Zazi, K. (2004). "Economic Analysis of Wind-Powered Desalination in the South of Morocco." *Desalination*, 165(0), 219-230.

APPENDICES

Appendix A: Bench-scale WindRO Basic Standard Operating Procedure

Night-before Preparation

- Make the salt solution
- If membrane is not already in DI water, cut coupon and place in DI water.

Cleaning (can be done in advance)

- The system should be sitting in DI from the previous run.
- Run the DI out until water level is just above pump.
- Fill small feed tank with 1 liter of 10% phosphoric acid (H_3PO_4) solution (117 ml of 85% H_3PO_4 added to DI water to make 1 liter).
- Run through for 20 minutes (10 minutes for H_3PO_4) in recycle mode to remove rust and particulates. (Note that after adding to DI, the acid concentration is lower than 10% and that is fine). Do not leave running much more than 20 minutes (15 minutes for H_3PO_4).
- Run through at least 28-l of DI water, without recycle.
- Make sure conductivity of the exit stream ends at close to the DI water -conductivity (one run had input of 25-mS DI water and output of 29-mS water. Other runs had input of less than 5-mS DI and output of around 8 or 9 mS).
- Leave system full of DI water.

Clean-water flux run

- DI should be in the system after the cleaning.

Calibrate conductivity meters. (50 mS for on-line meter, 0.447 mS for bench-top meter)

- Set up the system by bypassing the membrane cell and using 4-liter feed bottle.
- Calibrate computer clock.
- Tare pressure gauge. Don't tare flow meter; I think it drifts less than taring makes it change.
- Start "RO Control 31.vi"
- Run DI at high pressure. If pulsating, let it run at low pressure for several minutes, or run at about 300 psi, 7 Hz, until pulsation dampens. (Be sure that bubbles have left the DI before running.)
- Run the DI out until water level is just above pump (don't let air get into the pump).
- Add the solution of 74 g salt in 2 liters to the feed tank.
- Run system to mix salt with water already present. After mixing with the DI in the system, conductivity should be between 49 and 50 mS. If not, add a high-concentration salt solution, or DI water, as needed (again, let DI sit so air bubbles escape). Run until conductivity is between 49 and 50 mS.
- Take membrane coupon from DI water, place in cell with the 64 mil Osmonics feed spacer, pressurize to 1200 psi, and hook it up to the system. Note membrane type here: _____ .
- Remove water (to waste bucket) until the level is at the 1.5-L mark on the small bottle.

- Keep running system at 7 Hz (6.4 Hz on controller) with low pressure (concentrate valve completely open) and start computer data collection. This gives a flow rate through the Sepa cell of 800 ml/min, for a crossflow velocity (with the spacer) of 47 cm/sec.
- Write down file name and start time _____.
- Bring pressure up steadily for one or two minutes until it reaches 1000 psi on Labview.
- Using in-line permeate conductivity probe, record the permeate conductivity regularly, but especially toward the beginning. Ensure that proper rejection (at least 97%) is being achieved by the end of the clean-water flux run.
- At 1000 psi, the initial 50-µS sample should run at about 30 lmh.
- Run at constant 1000-psi pressure, 20˚C. Note that now this is the Labview reading and the gauge reading is about 1000, also. The display reading is about 985 psi. Check this and record: _____
- Adjust temperature control to keep it at 20 degrees C.
- Waste permeate until the feed reaches 70 mS/cm. It should take about 2.2 hours.

Turn off program, then shut down the pump.

Clean-water flux runII (if needed)

- This section uses a 24-hour period to compact the membrane.
- Remove most of the water in the system, down to the pump level, but do not run air through the pump.
- Fill feed tank up to 8-liter mark with an NaCl solution in DI water. This should be about 32 g/l NaCl (256 g total for the 8 liters). Adjust the concentration until it is at 50 mS/cm.
- Waste feed water through the system (send to waste bucket) to remove NaCl solution still in system. Waste about one liter bringing the feed water level to the 7-l mark.
- Connect tubing in recycle mode and start system at 6.96 Hz (6.4 Hz on controller). This gives a flow rate through the Sepa cell of 800 ml/min, for a crossflow velocity (with the spacer) of 47 cm/sec.
- Start computer data collection. Bring pressure up steadily for one or two minutes until it reaches 1000 psi.
- Write down file name and start time _____.
- Using in-line permeate conductivity probe, record the permeate conductivity regularly, but especially toward the beginning. Ensure that proper rejection (at least 98%) is being achieved.
- Run at constant 1000-psi pressure in recycle mode (permeate recycle, also) for 24 hours and observe flux decline.
- Monitor the feed-tank conductivity over time, ensuring that it remains constant.

Seawater (or sample of interest) runs without pressure vessel

- Bypass the pressure vessel
- Remove most of the water in the system, down to the pump level, but do not run air through the pump.
- Sample the feed, if needed.
- Get the sample to 20^{o}C in a water bath (if it is not already) and connect tube to the system. Place sample description here (concentration and conductivity):

  _____
- Fill feed tank up with 14L salt solution.
- Waste feed water through the system (send to waste bucket) to remove NaCl solution still in system. Waste 2 liter.
- Connect tubing in recycle mode and start system at 7 Hz (6.4 Hz on controller). This gives a flow rate through the Sepa cell of 800 ml/min, for a crossflow velocity (with the spacer) of 47 cm/sec.
- Start computer data collection. Bring pressure up steadily for one or two minutes until it reaches 1000 psi.
- Write down file name and start time

  _____.
- Make sure there is no bubble in in-line permeate conductivity probe, record the temperature regularly. Ensure that proper rejection (at least 98%) is being achieved.
- Run at constant 1000-psi pressure in recycle mode (permeate recycle, also) for 2 hours.
- Write down stop time, permeate mass, final feed conductivity and volume in the feed tank

  _____
- Sample for analytical methods according to the sampling plan, if there is one.
- Turn off program, and then shut down system.
- Run DI water through the system until water leaving the system has similar conductivity as water entering the system (one run had input of 25-µS DI water and output of 29-µS water. Other runs had input of less than 5-µS DI and output of around 8 or 9 µS, or even an output of 5-6 µS.)
- Start DI water run at 1000 psi for 30 mins. Write down the start, stop time and fluxes

  _____
- Leave system in DI water over night. Don't release the pressure on membrane cell, if you want to use the same membrane next time.
- Rinse conductivity probe with DI water. Leave to dry.
- Seawater (or sample of interest) runs with pressure vessel (no cross flow)
- Bypass the pressure vessel.
- Remove most of the water in the system, down to the pump level, but do not run air through the pump.
- Sample the feed, if needed.

- Get the sample to 20^{o}C in a water bath (if it is not already) and connect tube to the system. Place sample description here (conductivity and concentration): _____
- Fill feed tank up with 14 L solution.
- Turn all the sensors on.
- Start computer data collection. Write down file name and start time _____.
- Waste 2 L feed water through the system (send to waste bucket) to remove DI water in system.
- Connect the pressure vessel and tubing in recycle mode, close all the valves, besides the one between vessel and pump and start system at 7.0 Hz (6.4 Hz on controller). Fill the vessel with about 1 liter water.
- Connect to bypass mode and bring the pressure up to 500psi by adjusting the needle valve. (make sure this pressure is higher than air pressure below)
- At the same time, start pressurizing with nitrogen to 400 psi.
- Send water from pump to pressure vessel and close valve connected to membrane.
- Open valve for pressure vessel to membrane
- Close the needle valve
- Make sure that there is no bubble in in-line permeate conductivity probe and that proper rejection (at least 98%) is being achieved.
- Record the temperature to labview regularly.
- Adjusting the needle valve to make the pressure stay at 1000psi steady state for 2 hours.
- Write down the steady state start time:_____
- The excel file name which record volume of solution in feed tank: _____.
- Steady state stop time_____
- Close needle valve and the valve after pump and stop the pump at the same time.
- After 4 hours turn off the labview then shut down system.
- Write down the time stop the system _____
- Final pressure, rejection and conductivity in the feed tank: _____.
  Amount of permeate_____
- Measure the first a few ml of feed water after opening the needle valve. Be sure no gas goes through the membrane._____.
- Release the water and nitrogen in pressure vessel steadily.
- Connect in bypass mode and run DI water through the system until water leaving the system has similar conductivity as water entering the system (one run had input of 25-μS DI water and output of 29-μS water. Other runs had input of less than 5-μS DI and output of around 8 or 9 μS, or even an output of 5-6 μS.)
- Connect the pressure vessel and fill it by DI water (at least the same volume as salt water filled in it) for at least 1 time.

- Start DI water run at 1000 psi for 30 mins (by pass the P.V.). Write down the start, stop time and fluxes _____
- Leave system in DI water over night. Don't release the pressure on membrane cell, if you want to use the same membrane next time.
- Rinse conductivity probe with DI water. Leave to dry.

Seawater (or sample of interest) runs with pressure vessel (with cross flow)

- Bypass the pressure vessel.
- Remove most of the water in the system, down to the pump level, but do not run air through the pump.
- Sample the feed, if needed.
- Get the sample to 20^{o}C in a water bath (if it is not already) and connect tube to the system. Place sample description here (conductivity and concentration): _____
- Fill feed tank up with 14 L solution.
- Turn all the sensors on.
- Start computer data collection. Write down file name and start time _____.
- Waste 2 L feed water through the system (send to waste bucket) to remove DI water in system.
- Connect the pressure vessel and tubing in recycle mode, close all the valves, besides the one between vessel and pump and start system at 7.0 Hz (6.4 Hz on controller). Fill the vessel with about 1 liter water.
- Connect to bypass mode and bring the pressure up to 500psi by adjusting the needle valve. (make sure this pressure is higher than air pressure below)
- At the same time, start pressurizing with nitrogen to 400 psi.
- Send water from pump to pressure vessel and close valve connected to membrane.
- Open valve for pressure vessel to membrane
- Close the needle valve
- Make sure that there is no bubble in in-line permeate conductivity probe and that proper rejection (at least 98%) is being achieved.
- Record the temperature to labview regularly.
- Adjusting the needle valve to make the pressure stay at 1000psi steady state for 2 hours.
- Write down the steady state start time:_____
- The excel file name which record volume of solution in feed tank: _____.
- Steady state stop time_____
- Adjust the needle valve to reduce the pressure according to the experiment with PV and no cross flow.
- After 4 hours turn off the labview then shut down system.
- Write down the time stop the system _____

- Final pressure, rejection and conductivity in the feed tank: _____.
- Amount of permeate_____
- Measure the first a few ml of feed water after opening the needle valve. Be sure no gas goes through the membrane._____.
- Release the water and nitrogen in pressure vessel steadily.
- Connect in bypass mode and run DI water through the system until water leaving the system has similar conductivity as water entering the system (one run had input of 25-μS DI water and output of 29-μS water. Other runs had input of less than 5-μS DI and output of around 8 or 9 μS, or even an output of 5-6 μS.)
- Connect the pressure vessel and fill it by DI water (at least the same volume as salt water filled in it) for at least 1 time.
- Start DI water run at 1000 psi for 30 mins (by pass the P.V.). Write down the start, stop time and fluxes _____
- Leave system in DI water over night. Don't release the pressure on membrane cell, if you want to use the same membrane next time.
- Rinse conductivity probe with DI water. Leave to dry.

Appendix B: Matlab Data Analysis Programs

seeROdataClemsonYing01

```
%Developed by David Ladner and modified by Ying Sun

clear

%The following determines which plots to output. Set the "plots" array
%values to 1 to plot that plot, zero to not.
%plots = [1 1 1 1 1 1 1 1 1 1 1 1 1 1 1 1 1]; %This gives All plots
plots = [0 0 1 1 1 1 1 1 0 0 0 0 0 1 0 1 0]; %This gives monitoring
plots


%if you want to manually set opAdjust and Pwl, do it here and set
manParams
%to 1. To use parameters in files, set to 0.
manParams = 1;
if manParams ==1;
    opAdjust = 1.3;
    Pwl = 0.0084;
    opAdjustMan = 1.3;
    PwlMan = 0.0084;
end

%if the data are for seawater, set SWorNaCl to 1
%if the data are for NaCl, set SWorNaCl to 2
SWorNaCl = 2;

%if the data are for RO, set ROorNF to 1
%if the data are for NF, set ROorNF to 2
ROorNF = 1;

%set adjustFlow to 1 to correct flow meter calibration
adjustFlow = 0;

%Set filtering to 1 if you want to let the filterFlux subroutine go
through
%the permeate mass readings and calculate good flux values with linear
%fitting of portions of the mass readings.  This setting also lets the
%noise be plotted.  Set to 2 to supress the noise.
filtering = 1;

%set normalize to 1 if you want to plot the normalized flux value.  You
%have to give the value of the clean-water specific flux (in lmh/psi)
for this to work.
normalize = 0;

%set modelAdjust to 1 if you want to use film theory modeling to adjust
the
```

```
%specific flux.  Set to zero if you want to use bulk salt concentration
for specific
%flux calculation.
modelAdjust = 0;

filename = input('Enter Filename (with single quotes): ');
if strcmp(filename(1:4),'2006')
    pathname = 'C:\Dave\Research PhD\Bureau Project 2005-2006\Data\RO
Flux\2006\';
elseif strcmp(filename(1:4),'2007')
    pathname = 'C:\Dave\Research PhD\Bureau Project 2005-2006\Data\RO
Flux\2007\';
elseif strcmp(filename(1:4),'2008')
    pathname = 'C:\Dave\Research PhD\Bureau Project 2005-2006\Data\RO
Flux\2008\';
elseif strcmp(filename(1:4),'2009')
    pathname = 'C:\Dave\PostDoc\Data\RO\';
elseif strcmp(filename(1:4),'2010')
    pathname = 'C:\Dave\PostDoc\Data\RO\\';
elseif strcmp(filename(1:4),'2011')
    pathname = 'C:\Users\minniemouse\Desktop\research\RO data\';
elseif strcmp(filename(1:4),'2012')
    pathname = 'C:\Users\minniemouse\Desktop\research\RO data\';
end

if normalize == 1;
fid = fopen('C:\Dave\Research PhD\Bureau Project 2005-
2006\Data\2007\Matlab Programs\InitialFluxes.txt');
inifluxes = textscan(fid,'%s %f %f','delimiter',';');
index = find(strcmp(inifluxes{1},filename));
    if isempty(index) == 1;
        fprintf('No initial flux entry found. \n');
    else
        iniflux = inifluxes{2}(index);
    end
fclose(fid);
end

if normalize == 0;
    fprintf('Normalize: OFF \n');
elseif normalize ==1;
    fprintf('Normalize: ON \n');
end

if modelAdjust == 0;
    fprintf('Film Theory: OFF \n');
elseif modelAdjust ==1;
    fprintf('Film Theory: ON \n');
end

file = [pathname,filename];
```

```
if filtering == 1;
    fprintf('Filtering is ON, noise also shown \n');
elseif filtering ==2;
    fprintf('Filtering is ON, noise is HIDDEN \n');
else
    fprintf('Filtering is OFF \n');
end

data = load(file);
datasize = size(data);
if datasize(2)==5;
    if exist([file,'M.mat'],'file')==2;
    load([file,'M']);
    condPerm = (tdsPERMfull + 15.299)./512.1;
    Acond = (tdsCONCfull+664.62)./613.1;
    temp = tempSYSfull; clear tempSYSfull;
    clear tdsCONCfull; clear tdsPERMfull;
    pumpSpeed(1:length(temp)) = 0.1;
    Atime = AtimeHR./24;
    else
        fprintf('You must run arrangeData18 first. \n');
        return
    end
elseif datasize(2)==4;
    if exist([file,'M.mat'],'file')==2;
    load([file,'M']);
    condPerm = (tdsPERMfull + 15.299)./512.1;
    Acond = (tdsCONCfull+664.62)./613.1;
    clear tdsCONCfull; clear tdsPERMfull;
    temp = tempSYSfull; clear tempSYSfull;
    pumpSpeed(1:length(temp)) = 6.96;
    Atime = AtimeHR./24;
    else
        fprintf('You must run arrangeData18 first. \n');
        return
    end
else
Atime = data(2:length(data),1);
Acond = data(2:length(data),2);
Apressure = data(2:length(data),3);
ApermMass = data(2:length(data),4);
condPerm = data(2:length(data),5);
    %condPerm = voltPerm.*461.23 - 517.48; %this is before the permeate
probe is calibrated
temp = data(2:length(data),6);
Tankv = data(2:length(data),7);% saltwater volume in the feed tank
pumpSpeed = data(2:length(data),8);
clear data;
AtimeMIN = (Atime - Atime(1))*24*60;
AtimeHR = (Atime - Atime(1))*24;
clear AtimeMIN;
end
```

```
%filterFlux is a function to spit out the nice-looking and more
accurate
%flux data points

if filtering == 1 || filtering == 2;
[AtimeHRf, AfluxLMHf, filtInd] = filterFluxYing01(AtimeHR, ApermMass);

AcondF = Acond(filtInd);
ApressureF = Apressure(filtInd);
ApermMassF = ApermMass(filtInd);
%ApermCondF = ApermCond(filtInd);
tempF = temp(filtInd);
condPermF = condPerm(filtInd);
%pumpSpeedF = pumpSpeed(filtInd);
else
end

%The following converts grams per day into liters per meter squared per
hour
%This is based on the active membrane area in the cell being 0.01387
square
%meters (14.6 by 9.5 cm)
if filtering == 1 || filtering == 3;
%{
fdelta = 5;
%fdelta = input('Enter fdelta: ')
Aflux(1:fdelta)=0;
for j = fdelta+1:length(ApermMass);
    Aflux(j) = (ApermMass(j)-ApermMass(j-fdelta))./(Atime(j)-Atime(j-
fdelta));
end
%}
%Aflux = diff(ApermMass)./diff(Atime);
Aflux = diff(ApermMass)./mean(diff(Atime));
Aflux = [0 Aflux'];
AfluxLMH = Aflux./0.01387./1000./24; %gives the flux in liters per
meter squared per hour
else
end

%Now convert flow meter data to flux (ml/min to lmh), using a factor to
%calibrate the flow meter to the permeate mass flux data.
%this uses a separate file where names and calFact values are stored,
so
%that I don't have to do it every time.

%Convert conductivity to salt concentration.
if SWorNaCl == 1;
    tdsConc = Acond.*732.56 - 3831.6;  %converts conductivity (mS/cm)
to tds (mg/L) for Seawater
elseif SWorNaCl ==2;
    tdsConc = Acond.*759.6 - 5490.2;%tdsConc = Acond.*613.11 -
664.62;  %converts conductivity (mS/cm) to tds (mg/L) for NaCl
```

```
end
tdsPerm = condPerm.*512.1 - 15.30; %converts conductivity (mS/cm) to
tds (mg/L)
pumpSpeedF = pumpSpeed(filtInd);
tdsConcF = tdsConc(filtInd); %mg/L
tdsPermF = tdsPerm(filtInd); %mg/L
%in the following osmotic pressure calculations, a temperature
correction
%is used

if modelAdjust == 1;
    varyCP = 1;
    cpFactor = varyCP.*0.9975.*exp(0.005978.*AfluxLMH');
    cpFactor2 = varyCP.*0.9975.*exp(0.005978.*AfluxLMH2);
    cpFactorF = varyCP.*0.9975.*exp(0.005978.*AfluxLMHf');
elseif modelAdjust == 0;
    cpFactor = 1;
    cpFactor2 = 1;
    cpFactorF = 1;
end

tdsWall = tdsConc.*cpFactor;
tdsWall2 = tdsConc.*cpFactor2;
tdsWallF = tdsConcF.*cpFactorF;

%conversions used previously
%opConc = ((tdsWall./1000).^2*0.0374 + tdsWall./1000.*7.9875 +
0.4862).*(1+(temp-20).*0.0036); %converts mg/l to psi
%opConc2 = ((tdsWall2./1000).^2*0.0374 + tdsWall2./1000.*7.9875 +
0.4862).*(1+(temp-20).*0.0036); %converts mg/l to psi
%opConcF = ((tdsWallF./1000).^2*0.0374 + tdsWallF./1000.*7.9875 +
0.4862).*(1+(tempF-20).*0.0036); %converts mg/l to psi

%Seawater
%Conversions based on M. W. Kellogg Company, United States Office of
Saline
%Water, Saline water conversion engineering data book, U.S. Dept. of
the Interior, Washington, 1971
if SWorNaCl == 1;
    opConc = (1.416e-7.*tdsWall.^2 + 6.913e-2.*tdsWall -
80.64)./6.894757; %converts ppm to psi for seawater
    opConc2 = (1.416e-7.*tdsWall2.^2 + 6.913e-2.*tdsWall2 -
80.64)./6.894757; %converts ppm to psi for seawater
    opConcF = (1.416e-7.*tdsWallF.^2 + 6.913e-2.*tdsWallF -
80.64)./6.894757; %converts ppm to psi for seawater
elseif SWorNaCl ==2;
    opConc = (8.505e-2.*tdsWall - 86.61)./6.894757; %converts ppm to
psi for NaCl
    opConc2 = (8.505e-2.*tdsWall2 - 86.61)./6.894757; %converts ppm to
psi for NaCl
    opConcF = (8.505e-2.*tdsWallF - 86.61)./6.894757; %converts ppm to
psi for NaCl
end
```

```
opPerm =
(2*tdsPerm./1000./58.443.*1000.*8.314.*(temp+273)./1000./6.894757).*(1+
(temp-20).*0.0036); %converts mg/l to psi based on p = nRT/V
opPermF =
(2*tdsPermF./1000./58.443.*1000.*8.314.*(tempF+273)./1000./6.894757).*(
1+(tempF-20).*0.0036);

opAdjustMean = 1.28;
specFlux = AfluxLMH'./(Apressure - (opAdjustMean.*opConc-opPerm));
specFluxF = AfluxLMHf'./(ApressureF - (opAdjustMean.*opConcF-opPermF));
%specFluxFnoAdjust = AfluxLMHf'./(ApressureF - (opConcF-opPermF));
specFluxFnoAdjust = AfluxLMHf'./(ApressureF);

scrsz = get(0,'ScreenSize');
set(0,'defaulttextfontname','Arial');
set(0,'defaultaxesfontname','Arial');
set(0,'defaultaxesfontsize',12);

%Now we want to use our new model with Pwl and opAdjust to predict the
flux

if manParams == 0;
load coupParamsNM4;

index = find(strcmp(coupParamFiles,filename));
    if isempty(index) == 1;
    else
        Pwl = Pwls(index);
        opAdjust = opAdjusts(index);
    end

    fid = fopen('coupParamsManual.txt');
    coupParamsMan = textscan(fid,'%s %f %f','delimiter',';');
    fclose all;
    index2 = find(strcmp(coupParamsMan{1},filename));
    if isempty(index2) == 1;
        fprintf('No coupon parameter entries found, using 0.05 and 1.3
defaults \n');
        PwlMan = 0.05;
        opAdjustMan = 1.3;
    else
        PwlMan = coupParamsMan{2}(index2);
        opAdjustMan = coupParamsMan{3}(index2);
    end
end

fluxModel = Pwl.*(ApressureF-opAdjust.*(opConcF-opPermF));
fluxModelMan = PwlMan.*(ApressureF-opAdjustMan.*(opConcF-opPermF));

%Rej = 1-tdsPerm./tdsConc;
Rej = 1-(condPerm)./Acond;
```

```
iTankv = 12; % L, initial volume in the feed tank after waste 2 L feed
solution
% with 0 and 200 psi air pressure input, iTankv = 16, others, iTankv =
12
SaltWaterpv = iTankv - Tankv - ApermMass/1000; %L, volume of saltwater
in pv
Airpv = 10.68 - SaltWaterpv; % L, air volume in the pv
filebreaks = findstr(file,'\');
file = file(max(filebreaks)+1:length(file));

%These three lines are parameters for organizing plots on the screen.
incY = 0.04;
incX = 0.01;
k = 1;

if plots(k) == 1;
figure('Name',['Air volume in the pressure vessel
',file],'NumberTitle','off','Position',...
    [scrsz(3).*k.*incX scrsz(4).*(0.42-k*incY) scrsz(3)*.4
scrsz(4).*0.5])
%plot(AtimeMIN,AcfrMPS,'Color',[0 0 1])
plot(AtimeHR,Airpv,'Color',[0 0 1])
title(['air volume in the pressure vessel  ',file])
%xlabel('Time (min)')
xlabel('Time (hours)')
ylabel('Air volume (L)')
end
k = k+1;

if plots(k) == 1;
figure('Name',['water volume in the pressure vessel
',file],'NumberTitle','off',...
    'Position',[scrsz(3).*k.*incX scrsz(4).*(0.42-k*incY) scrsz(3)*.4
scrsz(4).*0.5])
plot(AtimeHR,SaltWaterpv,'Color',[0 0.2
0.7],'Linestyle','none','Marker','.','MarkerSize',5)
title(['water volume in the pressure vessel ',file])
xlabel('Time (hours)')
ylabel('water volume (L)')
end
k = k+1;

if plots(k) == 1;
figure('Name',['Conductivity ',file],'NumberTitle','off','Position',...
    [scrsz(3).*k.*incX scrsz(4).*(0.42-k*incY) scrsz(3)*.4
scrsz(4).*0.5])
%plot(AtimeMIN,AcfrMPS,'Color',[0 0 1])
plot(AtimeHR,Acond,'Color',[0 0 1])
hold on;
plot(AtimeHRf,AcondF,'o','Color',[1 0 0])
hold off;
title(['Conductivity  ',file])
%xlabel('Time (min)')
```

```
xlabel('Time (hours)')
ylabel('Conductivity (mS/cm)')
end
k = k+1;

if plots(k) == 1;
figure('Name',['Permeate Conductivity ',file],'NumberTitle','off',...
    'Position',[scrsz(3).*k.*incX scrsz(4).*(0.42-k*incY) scrsz(3)*.4
scrsz(4).*0.5])
plot(AtimeHR,condPerm,'Color',[0 0.2
0.7],'Linestyle','none','Marker','.','MarkerSize',5)
title(['Permeate Conductivity ',file])
xlabel('Time (hours)')
ylabel('Conductivity (mS/cm)')
end
k = k+1;

if plots(k) == 1;
figure('Name',['Pump Speed
',file],'NumberTitle','off','Position',[scrsz(3).*k.*incX
scrsz(4).*(0.42-k*incY) scrsz(3)*.4 scrsz(4).*0.5])
plot(AtimeHR,pumpSpeed,'Color',[0.2 0.1 0.5],'LineStyle','-
','Marker','.')
hold on;
plot(AtimeHRf,pumpSpeedF,'Color',[1 0
0],'LineStyle','none','Marker','o')
hold off;
title(['Pump Speed',file])
xlabel('Time (hours)')
ylabel('Hz')
end
k = k+1;

if plots(k) == 1;
figure('Name',['Temperature ',file],'NumberTitle','off',...
    'Position',[scrsz(3).*k.*incX scrsz(4).*(0.42-k*incY) scrsz(3)*.4
scrsz(4).*0.5])
plot(AtimeHR,temp,'Color',[0 0.2
0.7],'Linestyle','none','Marker','.','MarkerSize',5)
title(['Temperature ',file])
xlabel('Time (hours)')
ylabel('Temperature ^oC')
end
k = k+1;

if plots(k) == 1;
figure('Name',['Pressure
',file],'NumberTitle','off','Position',[scrsz(3).*k.*incX
scrsz(4).*(0.42-k*incY) scrsz(3)*.4 scrsz(4).*0.5])
%plot(AtimeMIN,Apressure,'Color',[0.8 0 0])
plot(AtimeHR,Apressure,'Color',[0.8 0 0])
hold on;
plot(AtimeHRf,ApressureF,'o','Color',[1 0 0])
```

```
hold off;
title(['Pressure  ',file])
%xlabel('Time (min)')
xlabel('Time (hours)')
ylabel('psi')
if ROorNF == 1;
%    set(gca,'Ylim',[960, 1040]);
elseif ROorNF ==2;
    set(gca,'Ylim',[200, 225]);
end
end
k = k+1;

if plots(k) == 1;
figure('Name',['Fluxes
',file],'NumberTitle','off','Position',[scrsz(3).*k.*incX
scrsz(4).*(0.42-k*incY) scrsz(3)*.4 scrsz(4).*0.5])
plot(AtimeHR,AfluxLMH,'Color',[1 0 0],'LineStyle','none','Marker','.')
hold on
plot(AtimeHRf,AfluxLMHf,'Color',[0 0.5
0],'LineStyle','none','Marker','.')
hold off
title(['Fluxes ',file])
set(gca,'FontSize',12)
%xlabel('Time (min)')
xlabel('Time (hours)')
ylabel('l/(m^2 x hour)')
%xlims = xlim; ylims = ylim; axis([0 xlims(2) 0 mode(AfluxLMH)*2])

xlims = xlim;
if ROorNF == 1;
    ylims = ylim; axis([0 xlims(2) 0 80]);
elseif ROorNF ==2;
    ylims = ylim; axis([0 xlims(2) 0 80]);
end

end
k = k+1;

%Now I want to plot the pressure with the osmotic pressure at the wall
if plots(k) == 1;
figure('Name',['Forces
',file],'NumberTitle','off','Position',[scrsz(3).*k.*incX
scrsz(4).*(0.42-k*incY) scrsz(3)*.4 scrsz(4).*0.5])
plot(AtimeHRf,ApressureF.*6.895,'.-r');
hold on;
plot(AtimeHRf,opConcF.*opAdjustMan.*6.895,'.-b');
plot(AtimeHRf,opConcF.*6.895,'.-g');
plot(AtimeHRf,ApressureF.*6.895-opConcF.*opAdjustMan.*6.895,'.-k');
hold off;
set(gca,'Ylim',[0 1200.*6.895]);
xlabel('Time (hours)');
ylabel('Pressure (kPa)');
```

```
legend('Applied','Wall Osmotic','Bulk Osmotic','Driving Force (dP-dPi)')
end
k = k+1;

if plots(k) == 1;
%figure('Name',['Flux Modeled
',file],'NumberTitle','off','Position',[scrsz(3).*k.*incX
scrsz(4).*(0.42-k*incY) scrsz(3)*.75 scrsz(4).*0.5])
figure('Name',['Flux Modeled
',file],'NumberTitle','off','Position',[scrsz(3).*k.*incX
scrsz(4).*(0.42-k*incY) 580 200])
hold on
%plot(AtimeHRf,fluxModel,'Color',[0 0 1],'LineStyle','-
','Marker','none')
plot(AtimeHRf,fluxModelMan,'Color',[0 0 0.9],'LineStyle','-
','Marker','none')
hold off
%title(['Fluxes ',file])
%set(gca,'FontSize',12)
%xlabel('Time (min)')
xlabel('Time (hours)')
ylabel('l/(m^2 x hour)')
%xlims = xlim; ylims = ylim; axis([0 xlims(2) 0 mode(AfluxLMH)*2])
xlims = xlim;
if ROorNF == 1;
    ylims = ylim; axis([0 xlims(2) 0 35]);
%    ylims = ylim; axis([0 xlims(2) 15 25]);
elseif ROorNF ==2;
    ylims = ylim; axis([0 xlims(2) 0 80]);
end
%legend('Data',['A = ',num2str(Pwl),', f_o_s = ',num2str(opAdjust)],...
%    ['A = ',num2str(Pwl),', f_o_s =
',num2str(opAdjust)],'Location','NorthEast');
%legend('Data',['A = ',num2str(Pwl),', f_o_s = ',num2str(opAdjust)],...
%    ['A = ',num2str(PwlMan),', f_o_s =
',num2str(opAdjustMan)],'Location','NorthEast');
toPrint = ['A = ',num2str(PwlMan),', f_o_s = ',num2str(opAdjustMan)];
text(10,23,toPrint);
legend boxoff;
box off;
end
k = k+1;

if plots(k) == 1;
figure('Name',['SpecFlux ',file],'NumberTitle','off',...
    'Position',[scrsz(3).*k.*incX scrsz(4).*(0.42-k*incY) scrsz(3)*.4
scrsz(4).*0.5])
plot(AtimeHR,specFlux./6.894757,'Color',[0 0.2
0.7],'Linestyle','none','Marker','.')
hold on;
plot(AtimeHRf,specFluxF./6.894757,'Color',[1 0
0],'LineStyle','none','Marker','o')
hold off;
```

```
title(['Specific Flux  ',file])
xlabel('Time (hours)')
ylabel('lmh/kPa')
if ROorNF == 1;
    set(gca,'Ylim',[0, max(specFluxF./6.894757).*1.2]);
end
end
k = k+1;

if plots(k) == 1;
figure('Name',['SpecFluxNoAdjust ',file],'NumberTitle','off',...
    'Position',[scrsz(3).*k.*incX scrsz(4).*(0.42-k*incY) scrsz(3)*.4
scrsz(4).*0.5])
%plot(AtimeHR,specFlux./6.894757,'Color',[0 0.2
0.7],'Linestyle','none','Marker','.')
hold on;
plot(AtimeHRf,specFluxFnoAdjust./6.894757,'Color',[1 0
0],'LineStyle','none','Marker','o')
hold off;
title(['Specific Flux No Adjust  ',file])
xlabel('Time (hours)')
ylabel('lmh/kPa')
if ROorNF == 1;
    set(gca,'Ylim',[0, max(specFluxFnoAdjust./6.894757).*1.2]);
end
end
k = k+1;

if plots(k) == 1;
if normalize == 1 && exist('iniflux','var') == 1;
figure('Name',['Normalized SpecFlux ',file],'NumberTitle','off',...
    'Position',[scrsz(3).*k.*incX scrsz(4).*(0.42-k*incY) scrsz(3)*.4
scrsz(4).*0.5])
normFlux = specFlux./iniflux;
normFluxF = specFluxF./iniflux;
plot(AtimeHR,normFlux,'Color',[0 0.2
0.7],'Linestyle','none','Marker','.')
hold on;
plot(AtimeHR,normFlux2,'Color',[0 0.7 0.2])
plot(AtimeHRf,normFluxF,'Color',[1  0  0],'LineStyle','none','Marker','o')
hold off;
title(['Normalized Specific Flux  ',file])
xlabel('Time (hours)')
set(gca,'Ylim',[0, 1.*1.2]);
end
end
k = k+1;

if plots(k) == 1;
if modelAdjust == 1;
    figure('Name',['cpFactorF ',file],'NumberTitle','off',...
    'Position',[scrsz(3).*k.*incX scrsz(4).*(0.42-k*incY) scrsz(3)*.4
scrsz(4).*0.5])
```

```
plot(AtimeHRf,cpFactorF);
k = k+1;

figure('Name',['Pressures',file],'NumberTitle','off',...
    'Position',[scrsz(3).*k.*incX scrsz(4).*(0.42-k*incY) scrsz(3)*.4
scrsz(4).*0.5])
plot(AtimeHRf,[ApressureF,opConcF])
legend('Applied Pressure','Osmotic Pressure')
end
end
k = k+1;

if plots(k) == 1;
figure;
hold on;
plot(AtimeHRf(2:end),AfluxLMHf(2:end)./max(AfluxLMHf),'Color',[1 0
0],'LineStyle','none','Marker','s')
plot(AtimeHRf(2:end),specFluxFnoAdjust(2:end)./6.894757./max(specFluxFn
oAdjust).*6.894757,'Color',[0 1 0],'LineStyle','none','Marker','^')
plot(AtimeHRf(2:end),specFluxF(2:end)./6.894757./max(specFluxF).*6.8947
57,'Color',[0 0 1],'LineStyle','none','Marker','d')
hold off;
end
k = k+1;

if plots(k) == 1;
    figure('Name',['Rejection',file],'NumberTitle','off',...
    'Position',[scrsz(3).*k.*incX scrsz(4).*(0.42-k*incY) scrsz(3)*.4
scrsz(4).*0.5])
    plot(AtimeHR,Rej,'s-');
    title(['Max Rej = ',num2str(max(Rej).*100),'   Final Rej =
',num2str(Rej(end).*100),'   Avg Rej = ',num2str(mean(Rej).*100)]);
end
k = k+1;

viscosity = 1e-6; %kPa-s
AfluxLMHfMS = AfluxLMHf.*2.7778e-7; %convert flux to m/s
Rtot = (ApressureF.*6.895-
opConcF.*opAdjustMan.*6.895)./(viscosity.*AfluxLMHfMS');

if plots(k) == 1;
    k2 = 1;
figure('Name',['Resistances
',file],'NumberTitle','off','Position',[scrsz(3).*k2.*incX
scrsz(4).*(0.42-k2*incY) scrsz(3)*.4 scrsz(4).*0.5])
plot(AtimeHRf,Rtot,'.-r');
hold on;
%plot(AtimeHRf,opConcF.*opAdjustMan.*6.895,'.-b');
%plot(AtimeHRf,opConcF.*6.895,'.-g');
%plot(AtimeHRf,ApressureF.*6.895-opConcF.*opAdjustMan.*6.895,'.-k');
hold off;
%set(gca,'Ylim',[0 1200.*6.895]);
xlabel('Time (hours)');
```

```
ylabel('Pressure (m^-^1)');
%legend('Applied','Wall Osmotic','Bulk Osmotic','Driving Force (dP-
dPi)')
legend('Rtot');
end
k = k+1;

save(['ROmatlabData/',file,'_processed']);
```

filterFluxYing01

```
%Developed by David Ladner and modified by Ying Sun
%Take balance data and filter out all the noise from beaker changes,
etc.
%Output the calculated flux info, with the time points of those flux
%values.

function [fitTime, AfluxLMHfilt, filtInd] = filterFlux(AtimeHR,
ApermMass)

clear divTrack
clear k
clear m
clear n
clear fitTime
clear mlPerHr
clear AfluxLMHnew

dApermMass = diff(ApermMass);
dAtimeHR = diff(AtimeHR);
cleanPoints = find(0< dApermMass & dApermMass < 4 & dAtimeHR > 0 &
dAtimeHR < 0.01);
%cleanPoints = find(0.3 < dApermMass & dApermMass < 5 & dAtimeHR >
0.004 & dAtimeHR < 0.005);

Aflux = diff(ApermMass)./mean(diff(AtimeHR));
Aflux = [0 Aflux'];
AfluxLMH = Aflux./0.01387./1000;

fitTime = AtimeHR(cleanPoints+1);
AfluxLMHfilt = AfluxLMH(cleanPoints+1);
filtInd = cleanPoints+1;
```

plotMultipleROpressure01

```
%Developed by David Ladner and modified by Ying Sun
%Plotting multiple RO data sets together
clear

%Matlab asks the user to select the first data file
[FileName, FilePath] = uigetfile('ROmatlabData\*.mat','Select processed
RO data file.');

newFile = ['ROmatlabData\',FileName];
load(newFile);

k=3;
figure('Name',['Fluxes
',FileName],'NumberTitle','off','Position',[scrsz(3).*k.*incX
scrsz(4).*(0.42-k*incY) scrsz(3)*.75 scrsz(4).*0.5])
plot(AtimeHR,Apressure,'Color',[1 0 0],'LineStyle','none','Marker','.')
hold on
title(['pressure ',file])
set(gca,'FontSize',12)
xlabel('Time (hours)')
ylabel('Flux (lmh)')
xlims = xlim;
ylims = ylim;
axis([0 xlims(2) 0 1100]);

colorSet = [0 0 1; 0 0.6 0; 0.5 0.1 0.5; 0.7 0.4 0.3; 0.1 0.1
0.1; .6 .6 0; 0 .6 .6; 1 0 0; 0 1 0; 0.1 0.5 0.1; 0.3 0.4 0.7; 0.2, 0.7,
0.8; 0.8, 0.9, 1; 0.2, 0.9, 0.1; 0.9,0.1, 0.2];


check = 1;
colorNum = 0;
while check == 1;
    colorNum = colorNum + 1;
%Matlab asks the user to select another data file
k = 3;
[FileName, FilePath] = uigetfile('ROmatlabData\*.mat','Select processed
RO data file.');
newFile2 = ['ROmatlabData\',FileName];
load(newFile2);

plot(AtimeHR,Apressure,'Color',colorSet(colorNum,:),'LineStyle','none',
'Marker','.')

%Ask the user if they want another plot
check = input('Would you like another data set plotted? (Type 1 for
yes): \n');

end
hold off;
```

plotMultipleROflux01

```
%Developed by David Ladner and modified by Ying Sun
%Plotting multiple RO data sets together
clear

%Matlab asks the user to select the first data file
[FileName, FilePath] = uigetfile('ROmatlabData\*.mat','Select processed
RO data file.');

newFile = ['ROmatlabData\',FileName];
load(newFile);

k=3;
figure('Name',['Fluxes
',FileName],'NumberTitle','off','Position',[scrsz(3).*k.*incX
scrsz(4).*(0.42-k*incY) scrsz(3)*.75 scrsz(4).*0.5])
plot(AtimeHR,AfluxLMH,'Color',[1 0 0],'LineStyle','none','Marker','.')
hold on
title(['Fluxes ',file])
set(gca,'FontSize',12)
xlabel('Time (hours)')
ylabel('Flux (lmh)')
xlims = xlim;
ylims = ylim;
axis([0 xlims(2) 0 80]);

colorSet = [0 0 1; 0 0.6 0; 0.5 0.1 0.5; 0.7 0.4 0.3; 0.1 0.1
0.1; .6 .6 0; 0 .6 .6; 1 0 0; 0 1 0; 0.1 0.5 0.1; 0.3 0.4 0.7; 0.2, 0.7,
0.8; 0.8, 0.9, 1; 0.2, 0.9, 0.1; 0.9,0.1, 0.2];


check = 1;
colorNum = 0;
while check == 1;
    colorNum = colorNum + 1;
%Matlab asks the user to select another data file
k = 3;
[FileName, FilePath] = uigetfile('ROmatlabData\*.mat','Select processed
RO data file.');
newFile2 = ['ROmatlabData\',FileName];
load(newFile2);

plot(AtimeHR,AfluxLMH,'Color',colorSet(colorNum,:),'LineStyle','none','
Marker','.')

%Ask the user if they want another plot
check = input('Would you like another data set plotted? (Type 1 for
yes): \n');

end
hold off;
```

plotMultipleROrejection01

```
%Developed by David Ladner and modified by Ying Sun
%Plotting multiple RO data sets together
clear

%Matlab asks the user to select the first data file
[FileName, FilePath] = uigetfile('ROmatlabData\*.mat','Select processed
RO data file.');

newFile = ['ROmatlabData\',FileName];
load(newFile);

k=3;
figure('Name',['Rejection
',FileName],'NumberTitle','off','Position',[scrsz(3).*k.*incX
scrsz(4).*(0.3-k*incY) scrsz(3)*.40 scrsz(4).*0.4])
plot(AtimeHR,Rej,'Color',[1 0 0],'LineStyle','none','Marker','.')
hold on
title(['Rejection ',file])
set(gca,'FontSize',12)
xlabel('Time (hours)')
ylabel('Rejection')
%xlims = xlim;
%ylims = ylim;
%axis([0 xlims(2) 0 80]);

colorSet = [0 0 1; 0 0.6 0; 0.5 0.1 0.5; 0.7 0.4 0.3; 0.1 0.1
0.1; .6 .6 0];


check = 1;
colorNum = 0;
while check == 1;
    colorNum = colorNum + 1;
%Matlab asks the user to select another data file
k = 3;
[FileName, FilePath] = uigetfile('ROmatlabData\*.mat','Select processed
RO data file.');
newFile2 = ['ROmatlabData\',FileName];
load(newFile2);

plot(AtimeHR,Rej,'Color',colorSet(colorNum,:),'LineStyle','none','Marke
r','.')

%Ask the user if they want another plot
check = input('Would you like another data set plotted? (Type 1 for
yes): \n');

end

hold off;
```